



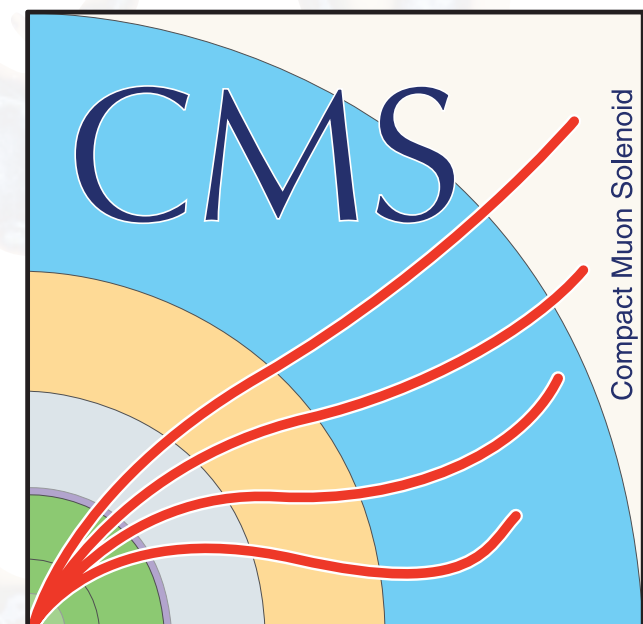
Higgs results from the combination at ATLAS and at CMS.

Jim Lacey

on behalf of the ATLAS and CMS collaborations

QCD@LHC 2017, Debrecen (Hungary)

Aug 29, 2017



Talk focuses on the mass, cross sections and couplings measurements from the ATLAS Run-2 combination and the ATLAS+CMS Run-I combination

- Introduction
- Higgs boson mass combination
- Higgs boson signal strength, cross sections and couplings combination
- Conclusions and outlook

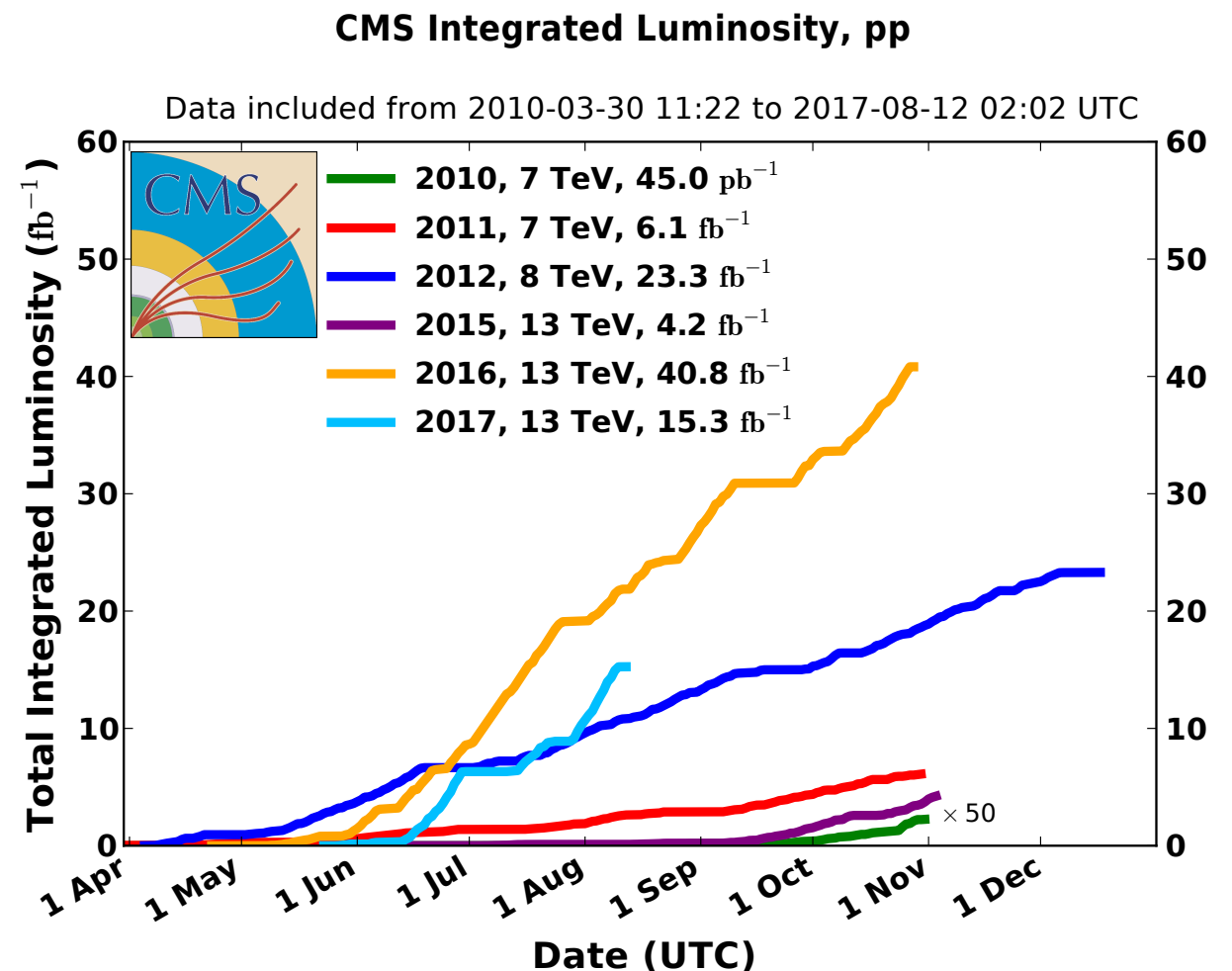
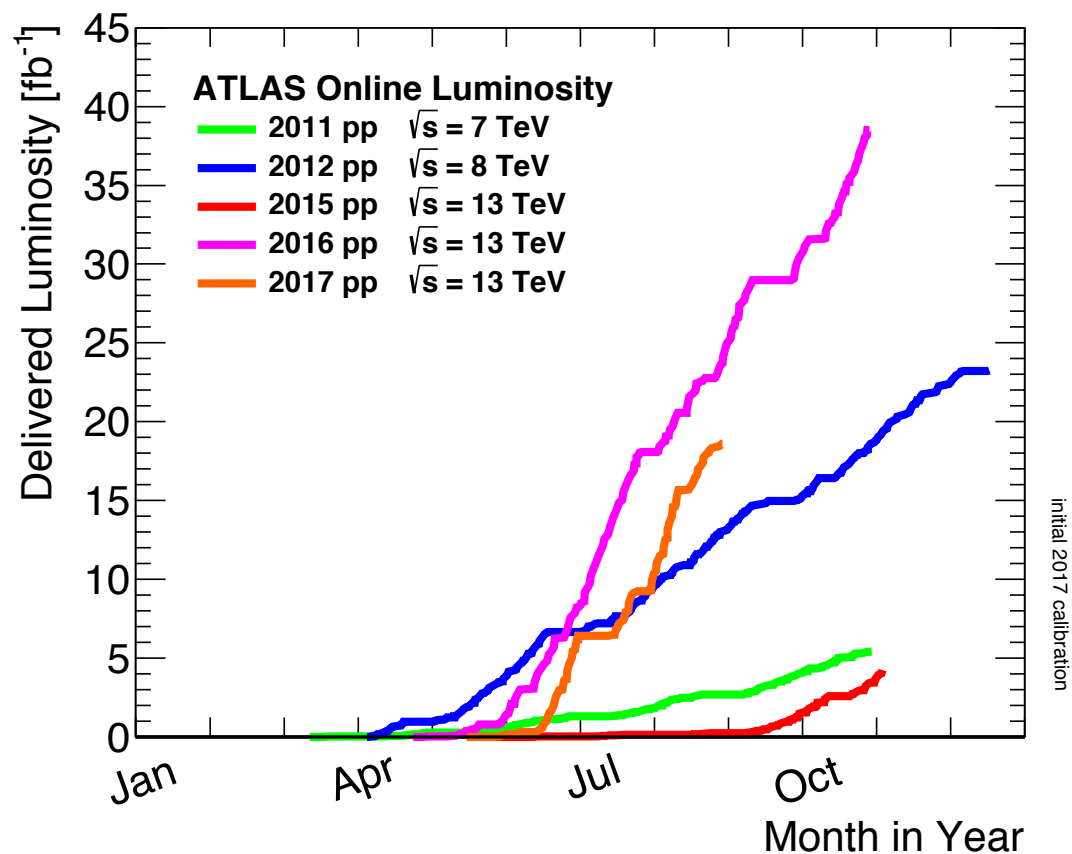
LHC performed very well during Run-1 and Run-2

Both ATLAS and CMS experiments achieved very *high data taking efficiencies*

~90% of data ready for physics

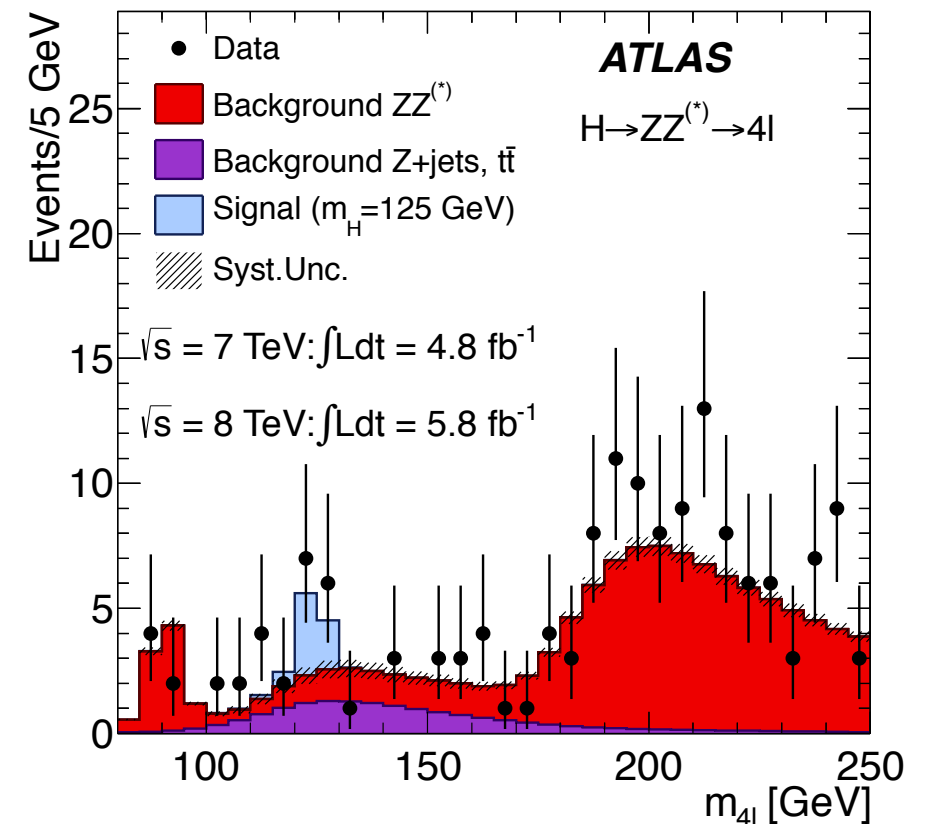
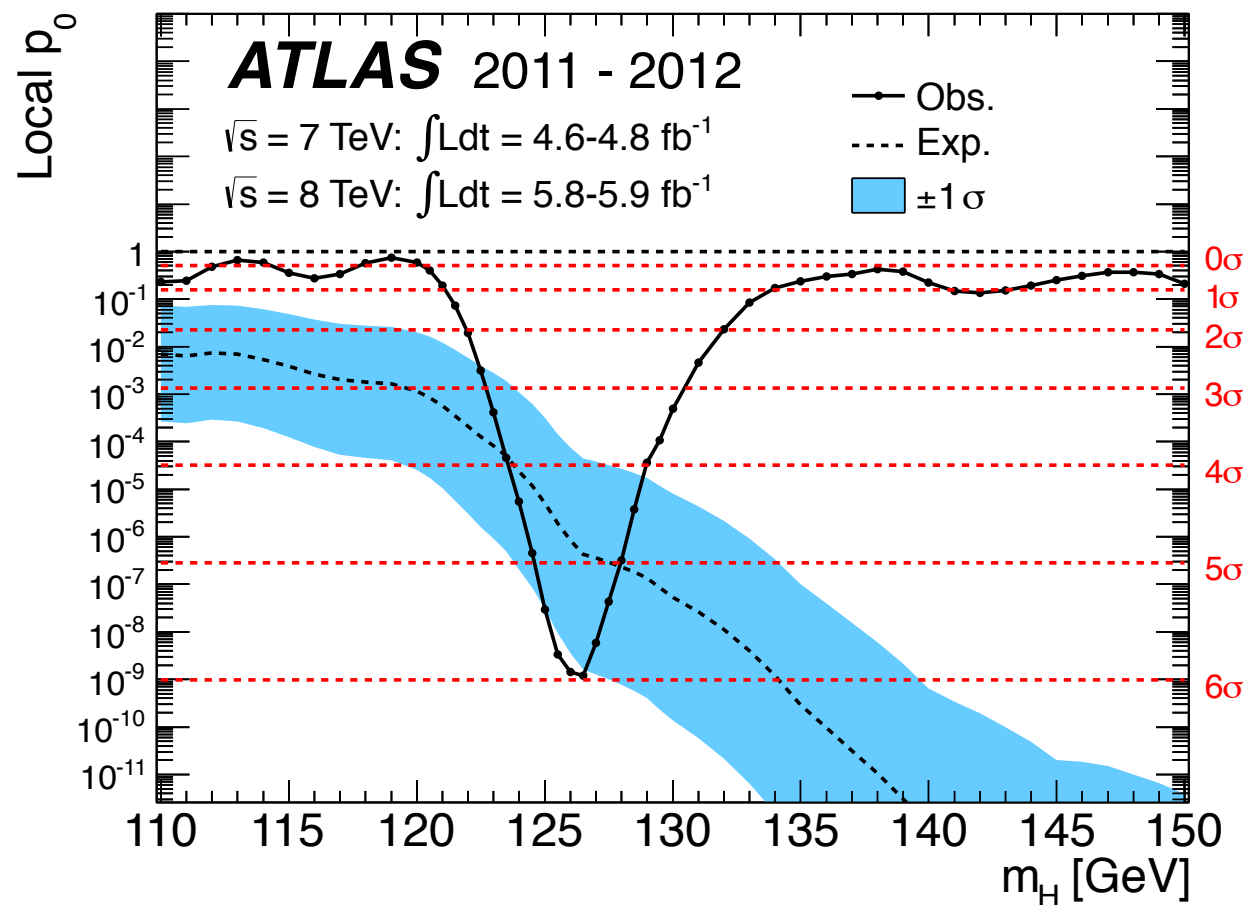
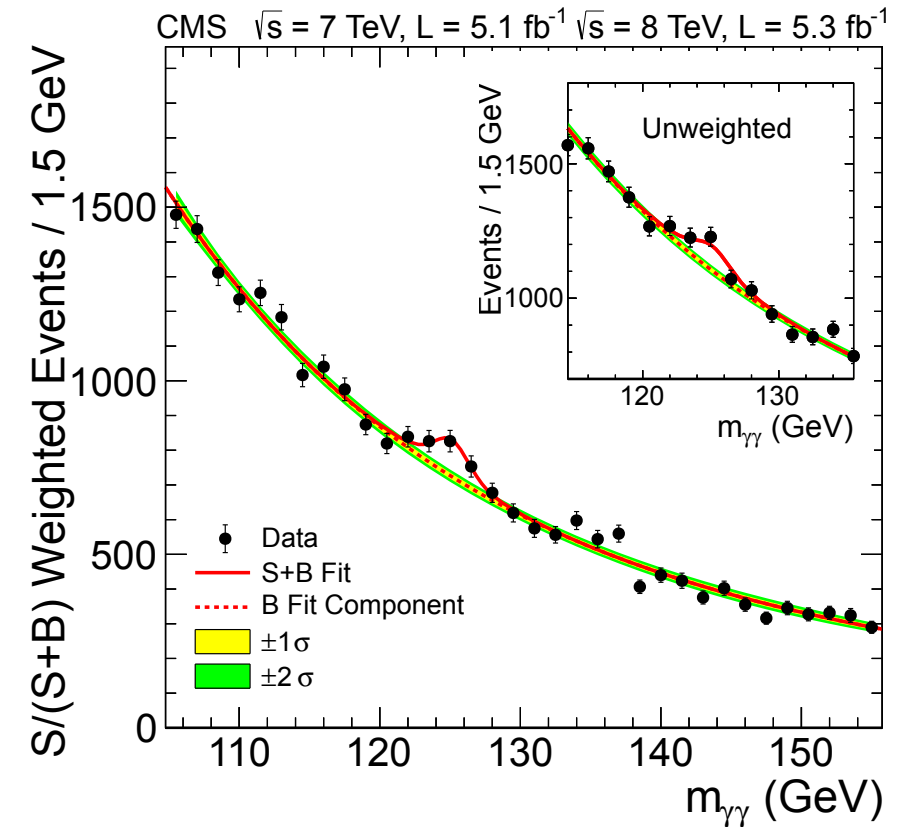
Data for analysis:

- 2011: $\sqrt{s}=7$ TeV: ~ 5 fb⁻¹
- 2012: $\sqrt{s}=8$ TeV: ~ 20 fb⁻¹
- 2015 & 2016: $\sqrt{s}=13$ TeV: ~ 36 fb⁻¹

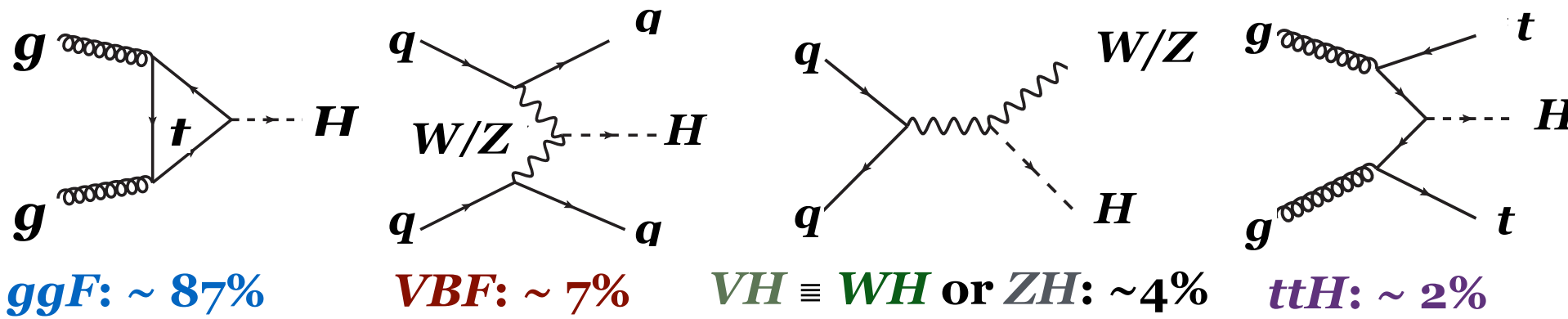


Higgs Discovery: July 2012.

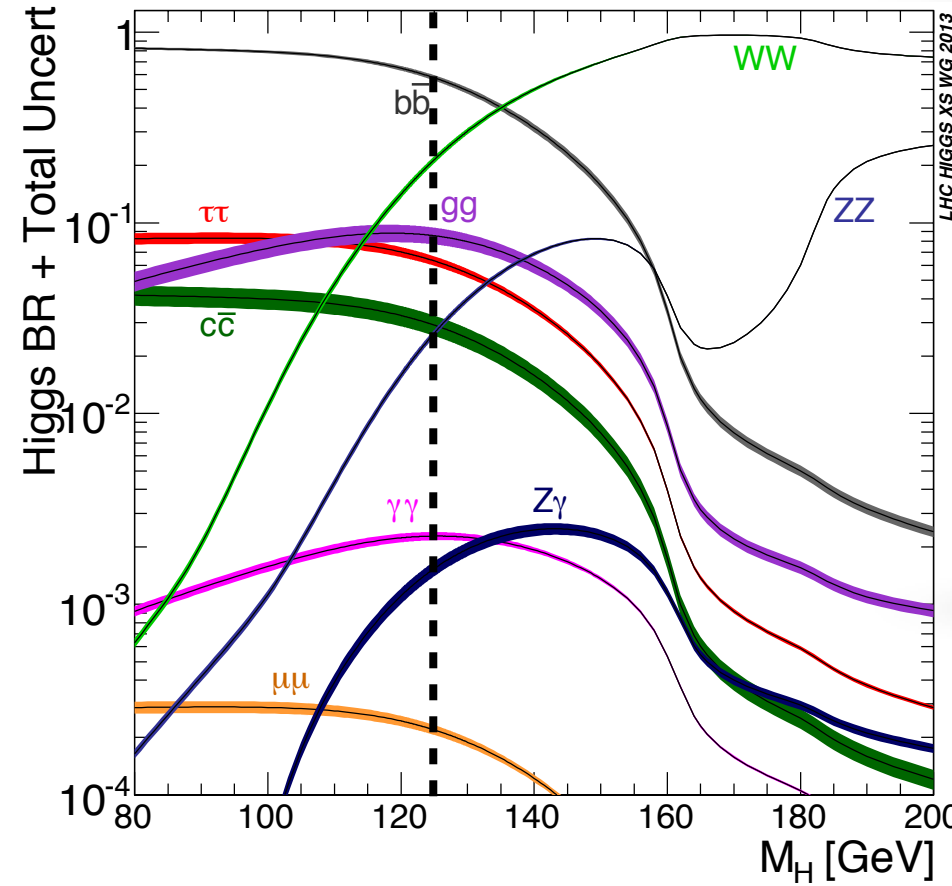
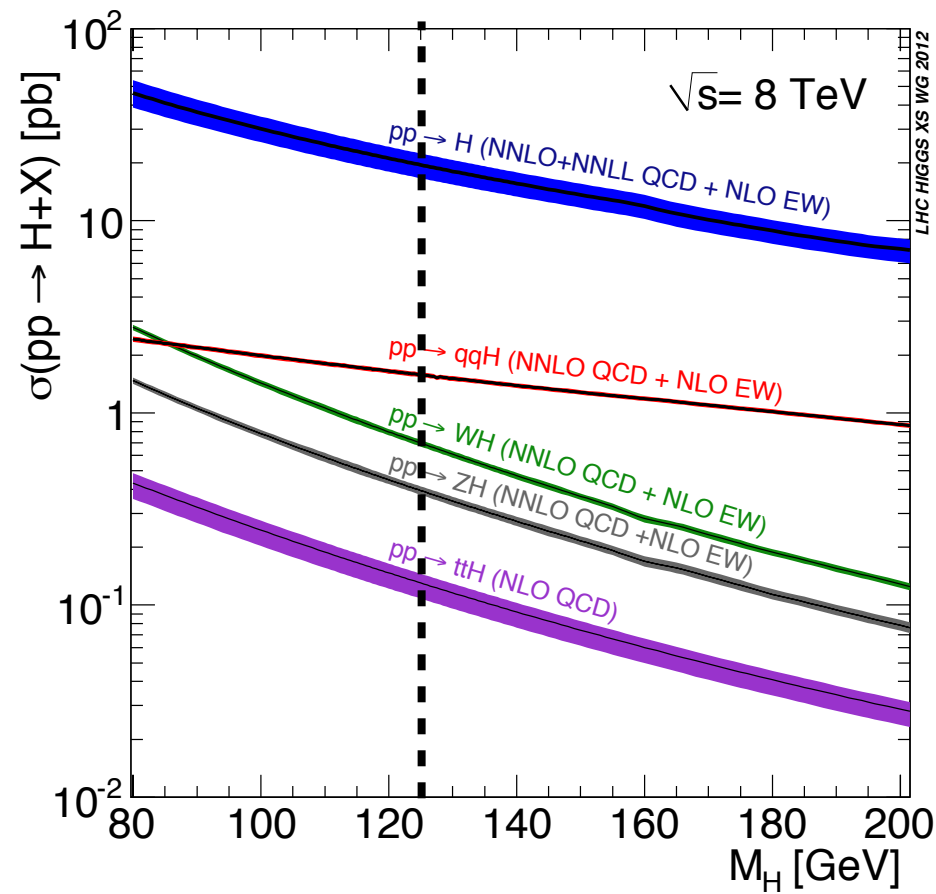
- Crowning achievement of Run 1
- To determine whether the discovered boson is *fully compatible* with the Standard Model Higgs, precise property measurements are required
 - Large effort towards studying its properties and searching for NP



Higgs boson production & decay.



bbH and $gg \rightarrow ZH$
 not targeted by
 specific analysis
 categories
 implemented in
 the fit model



**No dedicated
 analyses for
 $H \rightarrow cc$ or $H \rightarrow gg$
 (S/B too low)**

Before making a **statement** on the SM nature of the Higgs, we first need m_H
 Once the mass is determined then **all other properties** of the Higgs boson are
set and calculable

Combine measurements and fit for parameters of interest (POI) using a profile likelihood ratio:

$$\Lambda = \frac{L(\vec{\alpha}, \hat{\vec{\theta}}(\vec{\alpha}))}{L(\hat{\vec{\alpha}}, \hat{\vec{\theta}})}$$

- $\vec{\alpha}$: a vector of POI
- $\vec{\theta}$: nuisance parameters (NP), corresponding to systematic uncertainties
- $\vec{\alpha}, \vec{\theta}$ are the values of the POI and NP that maximize L
- $\hat{\vec{\theta}}(\vec{\alpha})$ is the value of the NP that maximize L for a given $\vec{\alpha}$
- Assume asymptotic approximation to be valid: $f(\Lambda) = \chi^2(ndof)$

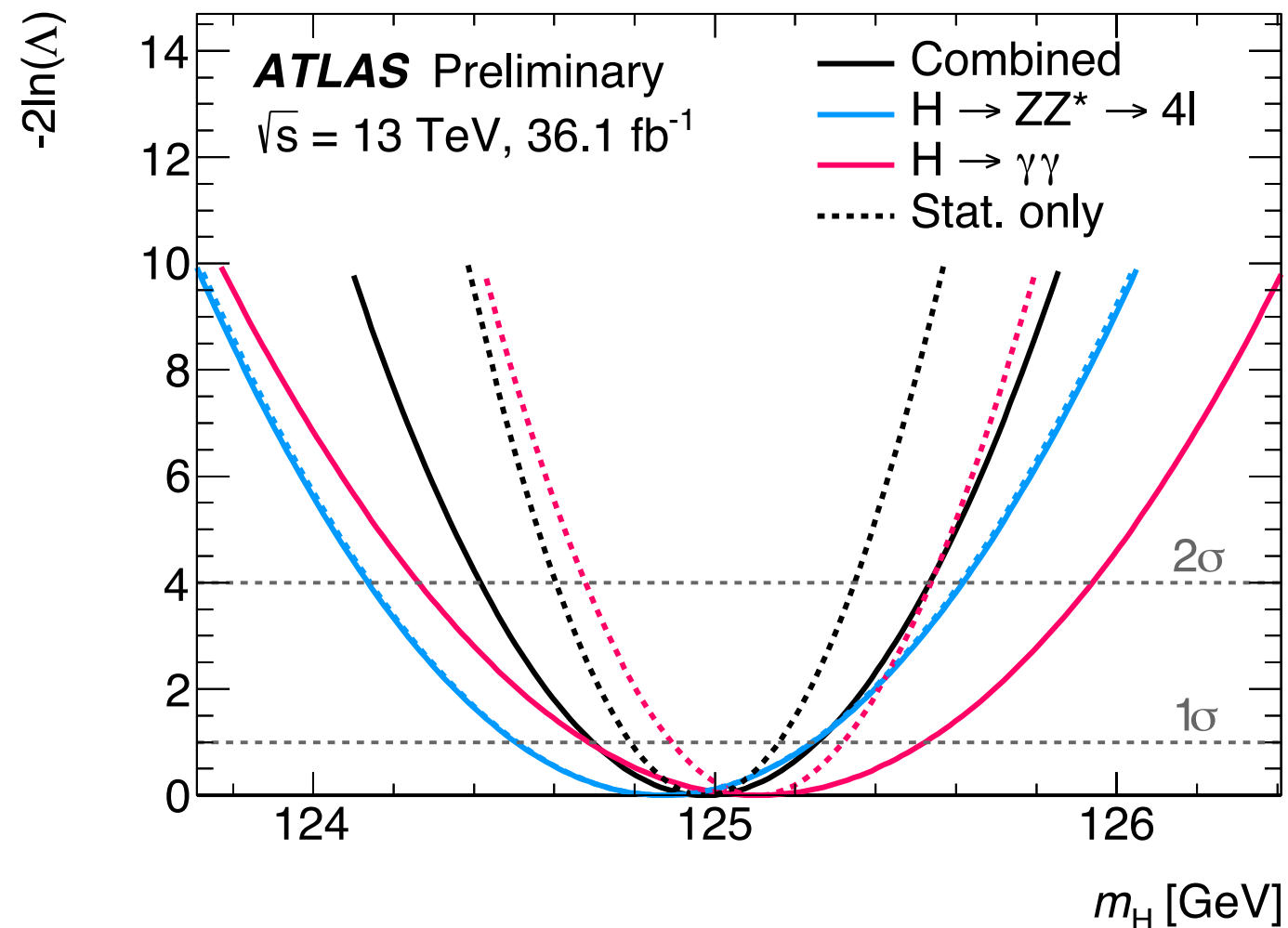
Theory uncertainties assumed *uncorrelated between production modes* (*except for VBF+VH*) and *correlated* between the two experiments

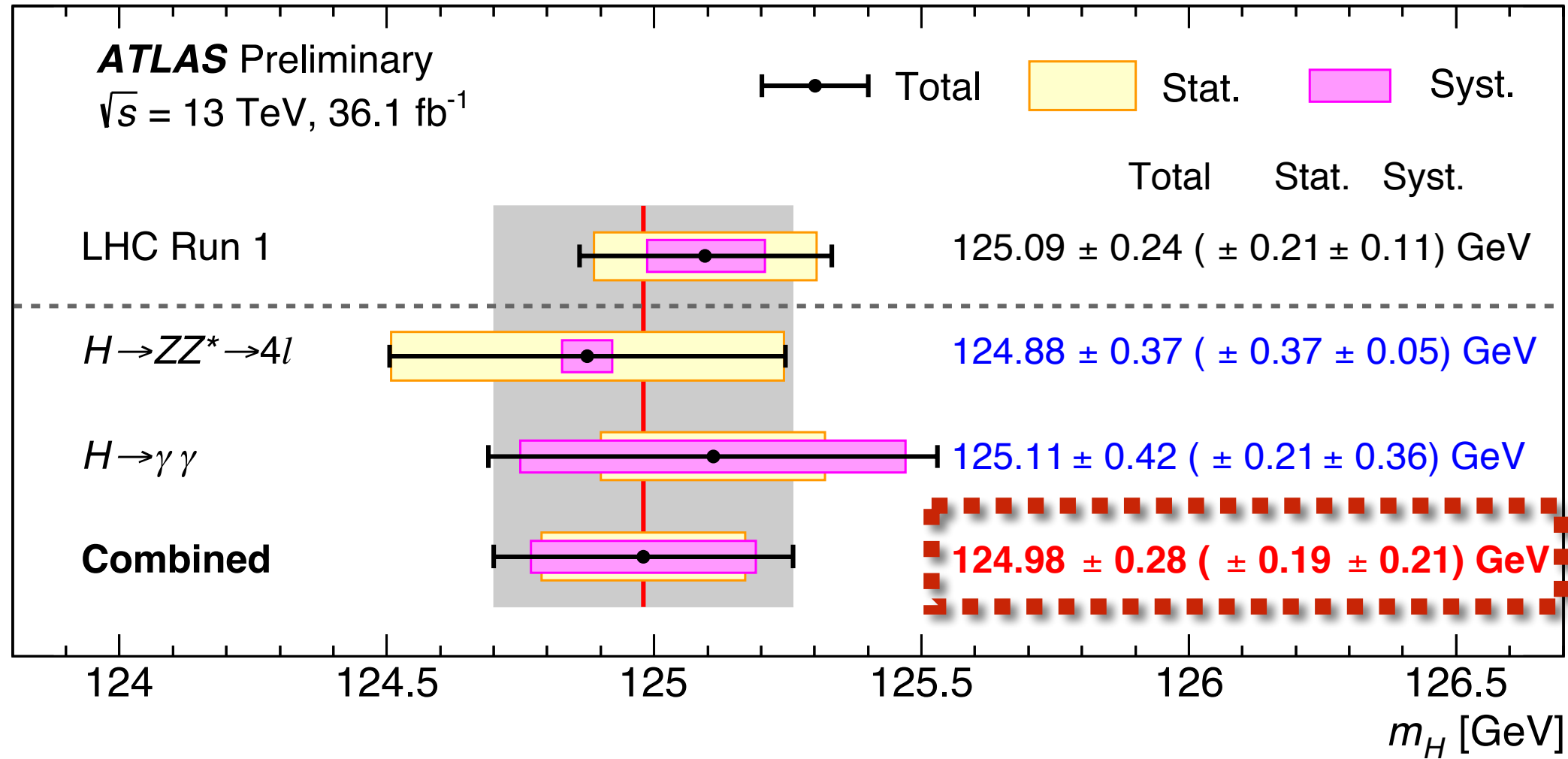
QCD, PDF, UEPS, B^f

Experimental uncertainties are *correlated between analysis channels* but *uncorrelated between the two experiments, except for part of the luminosity*

Higgs boson mass

- Combining measurements in $H \rightarrow \gamma\gamma$ and $H \rightarrow 4l$ decay channels
channels have the best mass resolution
- **Neglect interference** between $gg \rightarrow \gamma\gamma$ and $gg \rightarrow H \rightarrow \gamma\gamma$:
$$\Delta m_{\gamma\gamma} = -35 \pm 9 \text{ MeV (ATLAS)}$$
- Use profile likelihood ratio

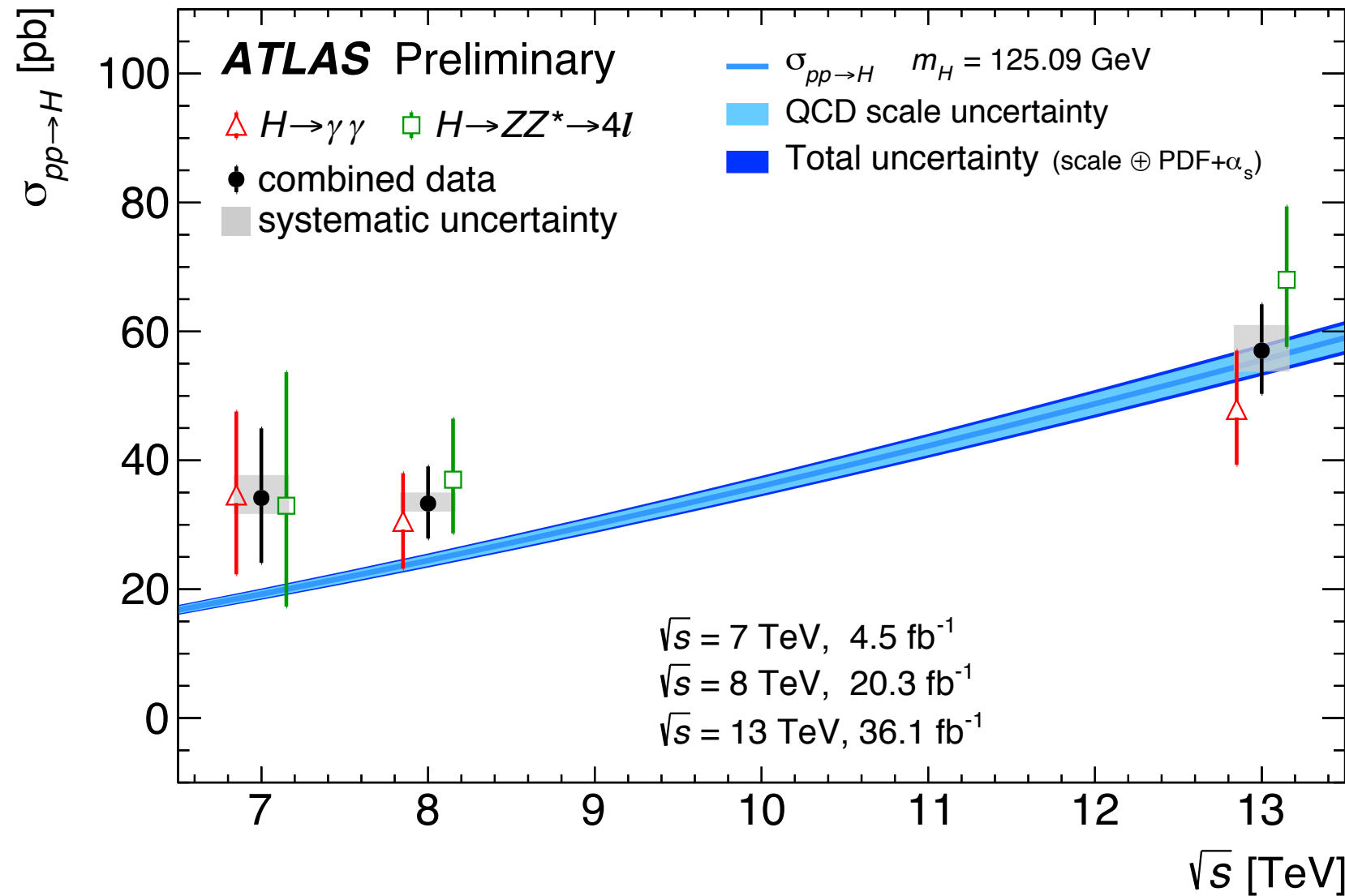




Source	Systematic uncertainty on m_H [MeV]
LAr cell non-linearity	90
LAr layer calibration	90
Non-ID material	60
ID material	50
Lateral shower shape	50
$Z \rightarrow ee$ calibration	30
Muon momentum scale	20
Conversion reconstruction	20

ATLAS combined mass in **excellent agreement with the LHC Run-1 average**

Higgs boson cross sections, signal strengths and couplings



Total cross section based on inclusive yields in each decay channel

- Yields extracted via a *fit to the inclusive mass distributions* ($m_{\gamma\gamma}$ and m_{4l})
- Corrections for: detector effects, fiducial acceptances, BR

Individual channel compatibility: p -value = 29%

Compatibility with SM: p -value = 84%

To increase sensitivity most analyses **split datasets into categories**

- Categories have different S/B and background uncertainties
- Many categories provide **sensitivity to different production modes**

Categories receive contributions from different productions and decay processes and encode information about different couplings

	Run-1 ATLAS+CMS		13 TeV ATLAS			
	ggF	VBF	VH	ttH		
$H \rightarrow \gamma\gamma$	✓ ✓	✓ ✓	✓ ✓	✓ ✓	✓ ✓	
$H \rightarrow ZZ^* \rightarrow 4l$	✓ ✓	✓ ✓	✓ ✓	✓ ✓	✓ ✓	
$H \rightarrow WW \rightarrow 2l2\nu$	✓ ✗	✓ ✗	✓ ✗	✓ ✗	✓ ✗	
$H \rightarrow \tau\tau$	✓ ✗	✓ ✗	✓ ✗	✓ ✗	✓ ✗	
$H \rightarrow bb$	✗ ✗	✗ ✗	✓ ✗	✓ ✗	✓ ✗	
$H \rightarrow \mu\mu$	✓ ✗	✓ ✗	✗ ✗	✗ ✗	✗ ✗	

S/B too low in $gg \rightarrow H \rightarrow bb$

ATLAS+CMS Run-1

- ▶ VBF $H \rightarrow bb$ (CMS) not included
- ▶ $H \rightarrow \mu\mu$ N_{sig} too low for **VH ttH**

$H \rightarrow \mu\mu$ used only in one model

ATLAS Run-2

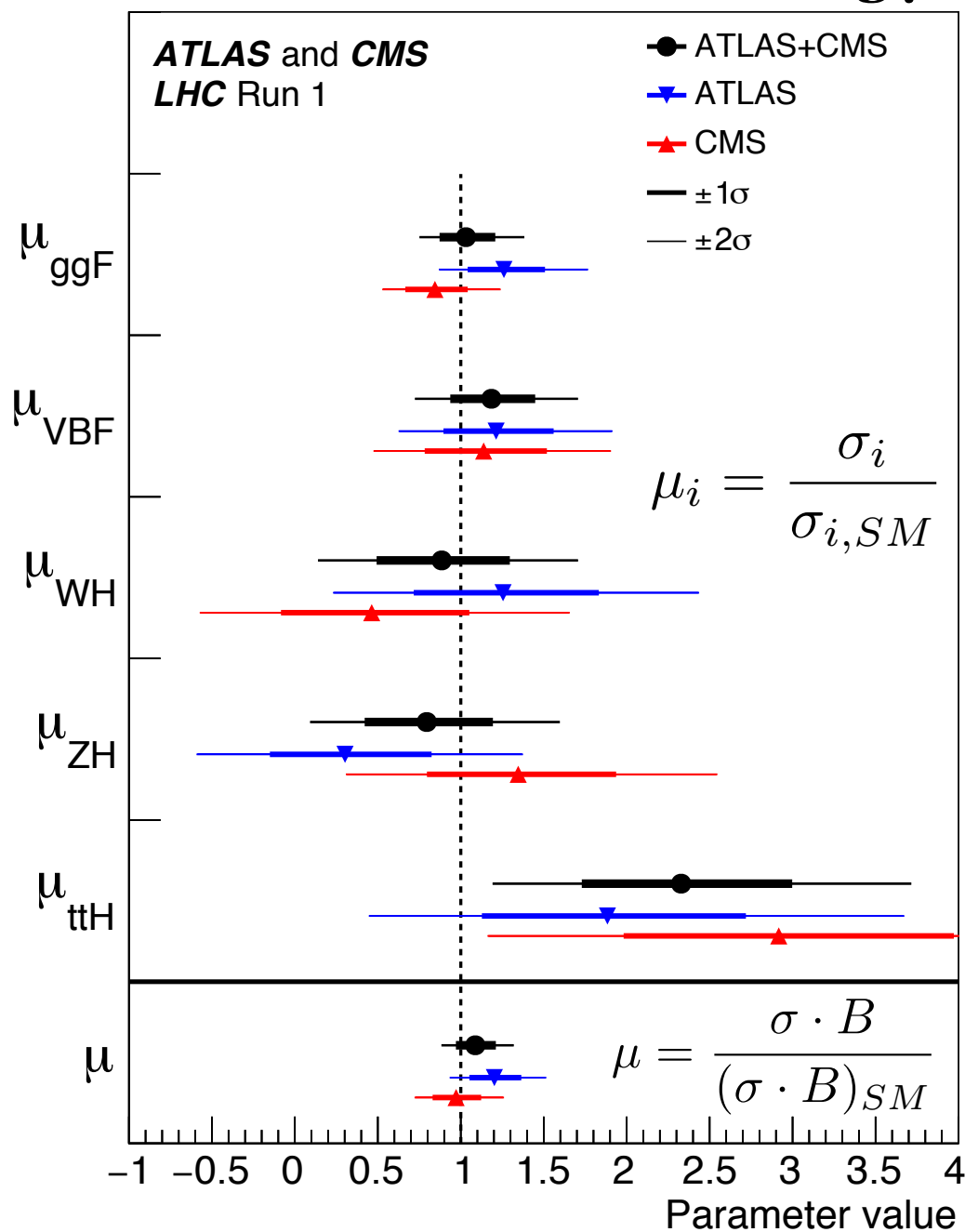
- ▶ considering only $H \rightarrow \gamma\gamma$ and $H \rightarrow 4l$

Assumptions:

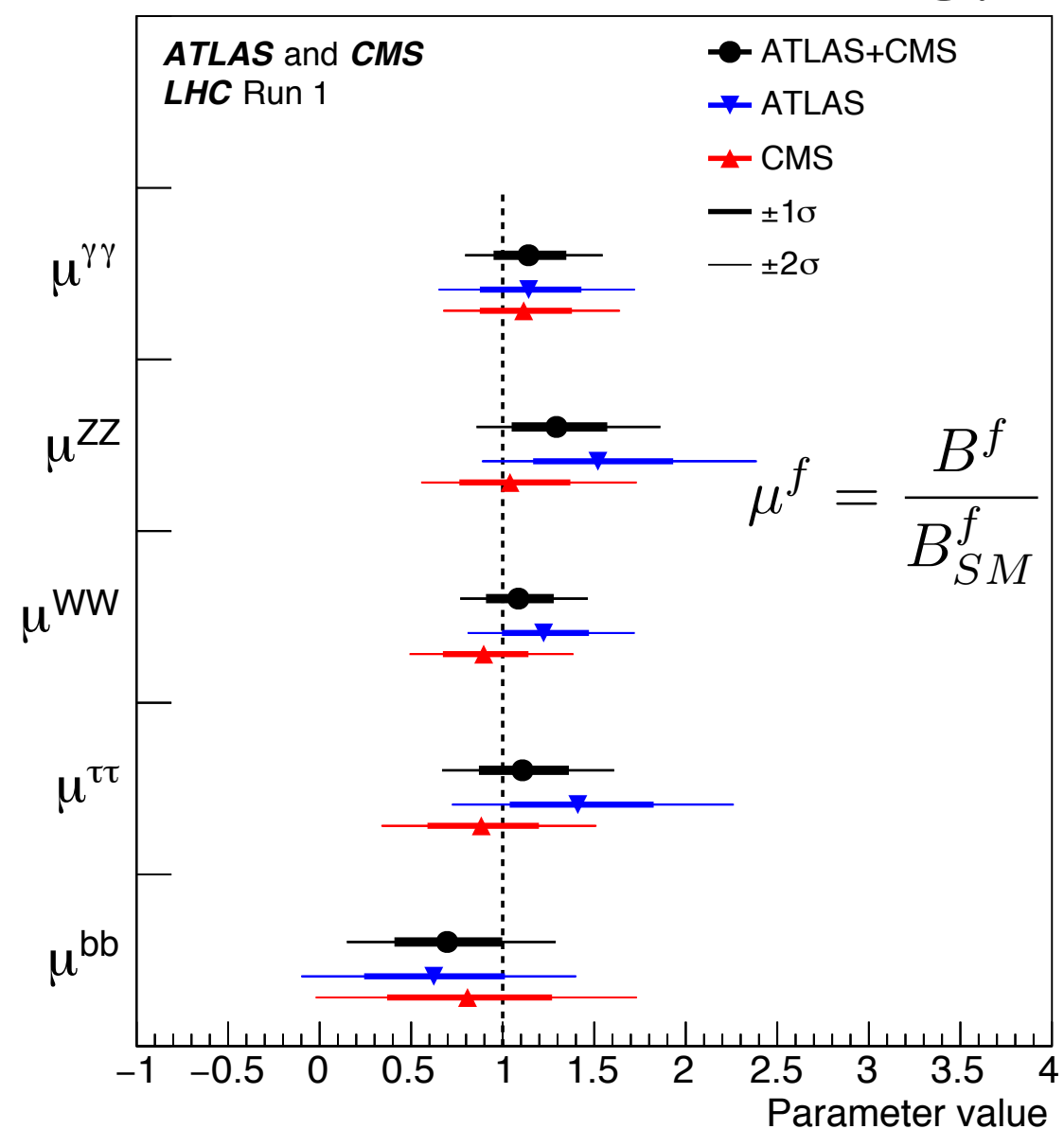
- **Single Higgs boson, CP-even, SM kinematics**
- **Narrow Width Approximation (NWA: $\Gamma_H \sim 4 \text{ MeV}$)**

$$\sigma(i \rightarrow H \rightarrow f) = \sigma_i \frac{\Gamma_f}{\Gamma_{\text{tot}}}$$

B^f set to SM when measuring μ_i



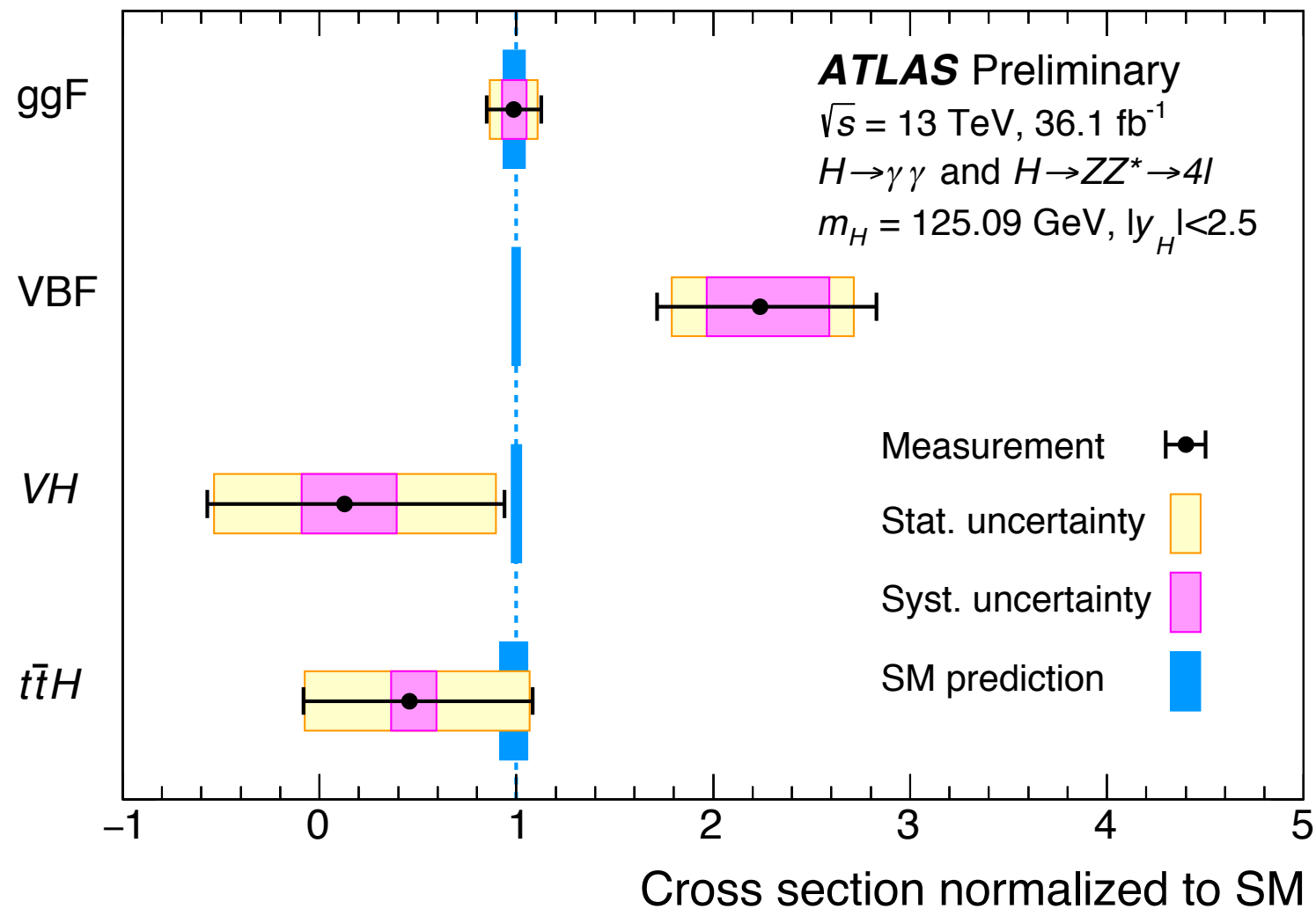
σ_i set to SM when measuring μ^f



ATLAS+CMS Run-1: $\mu = 1.09 \pm 0.07(stat.) \pm 0.05(exp.) \pm 0.03(th. B) \pm 0.07(th. S)$

ATLAS 13 TeV: $\mu = 1.09 \pm 0.09(stat.) \pm 0.06(exp.) \pm 0.06(th.)$

All *production and decay signal strength* measurements *consistent with SM*



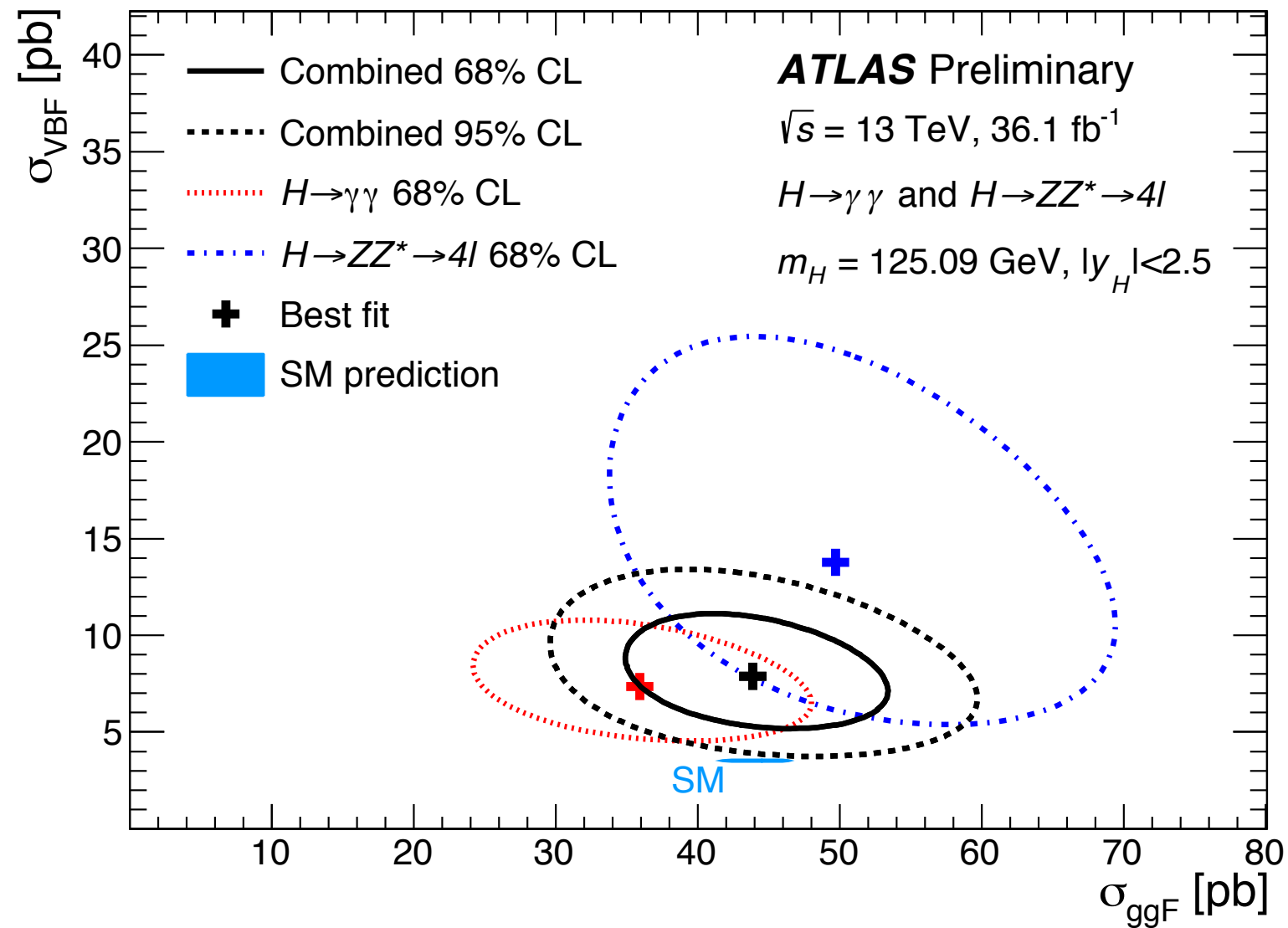
Higgs production is studied further by separating the production mechanism cross sections

Assuming SM branching fractions, a combined fit is performed, to extract the production cross sections (ggF , VBF , VH , and $t\bar{t}H$) for $|y_H| < 2.5$

Measurements of ggF and $t\bar{t}H$ include bbH and tH , respectively

Compatibility with SM predictions: $p\text{-value} = 5\%$

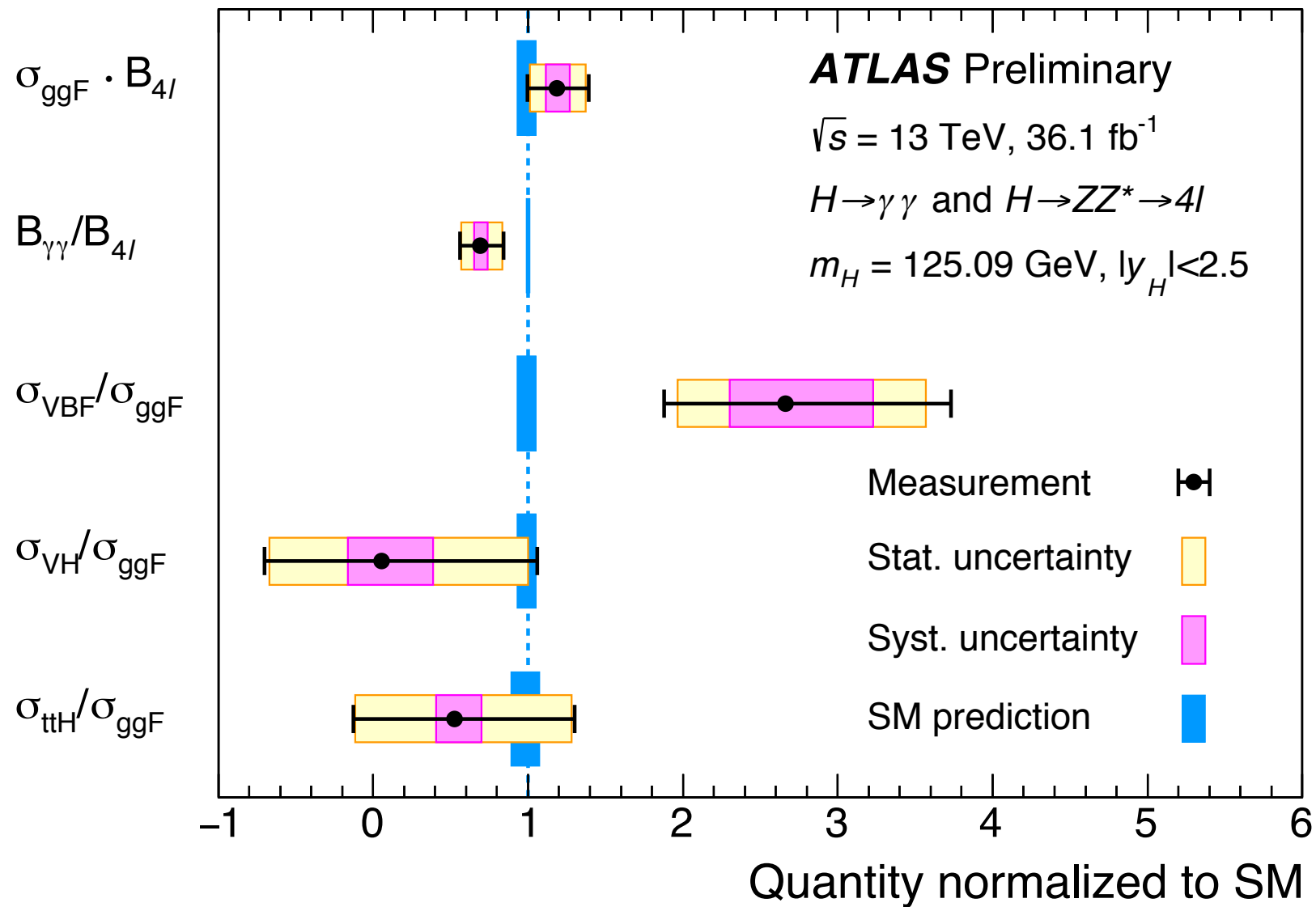
ggF and **VBF** cross sections measured with the best precision
Anti-correlated since the **VBF selection categories have significant contribution from ggF** production



2D compatibility with SM predictions:
p-value = 3%

$\sigma(\text{VBF})$ vs. $\sigma(\text{ggF})$ likelihood contours for each analysis channel and their combination (VH and ttH profiled with the data)

13 TeV $H \rightarrow \gamma\gamma + H \rightarrow 4l$ cross section ratios.



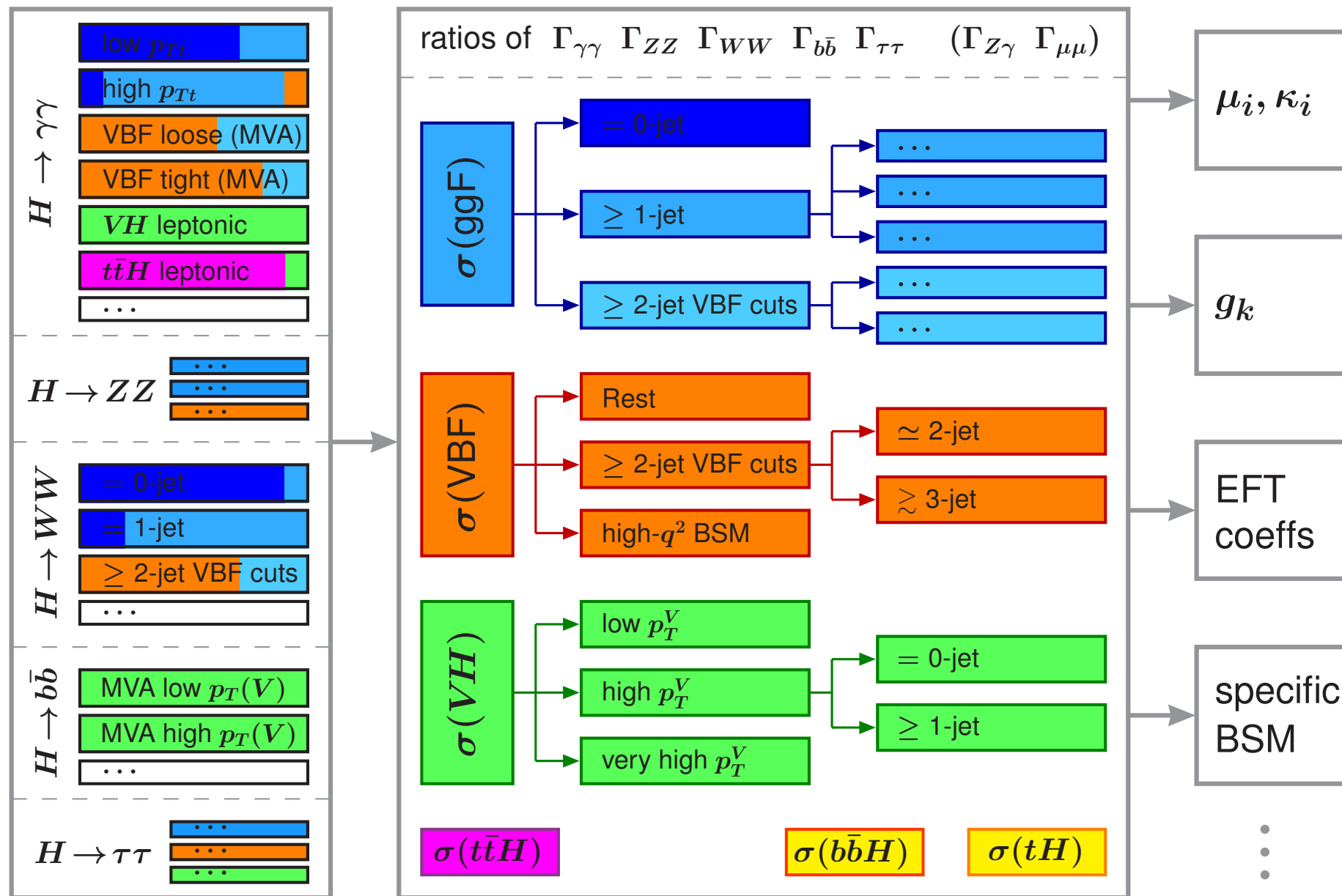
VBF, VH, and ttH normalized to ggF and $B^{\gamma\gamma}$ normalized to B^{ZZ}

$$\sigma_i \cdot B^f = \sigma(gg \rightarrow H \rightarrow ZZ) \cdot \left(\frac{\sigma_i}{\sigma_{ggF}} \right) \cdot \left(\frac{B^f}{B^{ZZ}} \right)$$

Combined fit to extract the production and decay ratios for $|y_H| < 2.5$

Compatibility with SM predictions: **p-value = 3%**

STXS framework ($|y_H| < 2.5$).



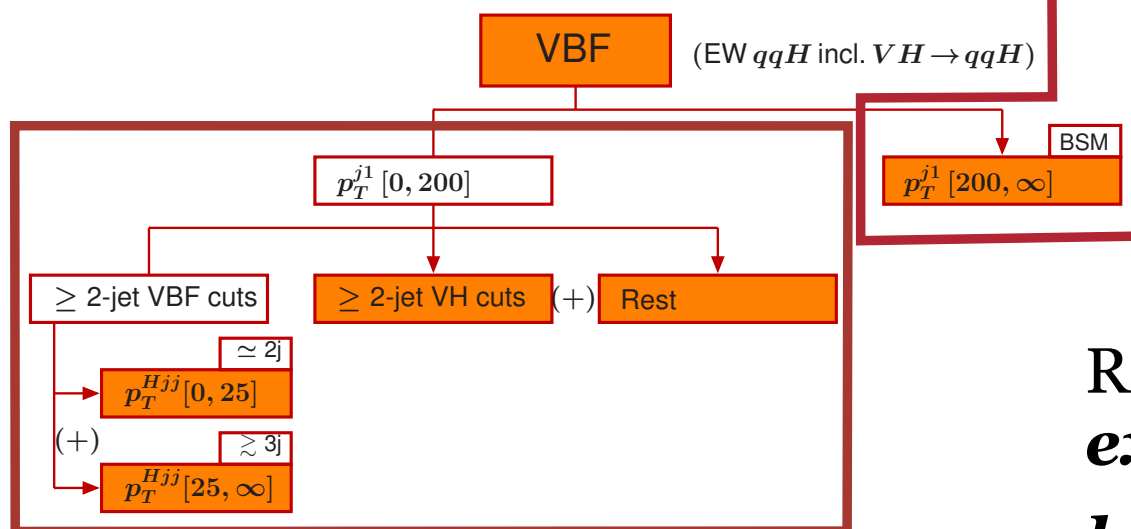
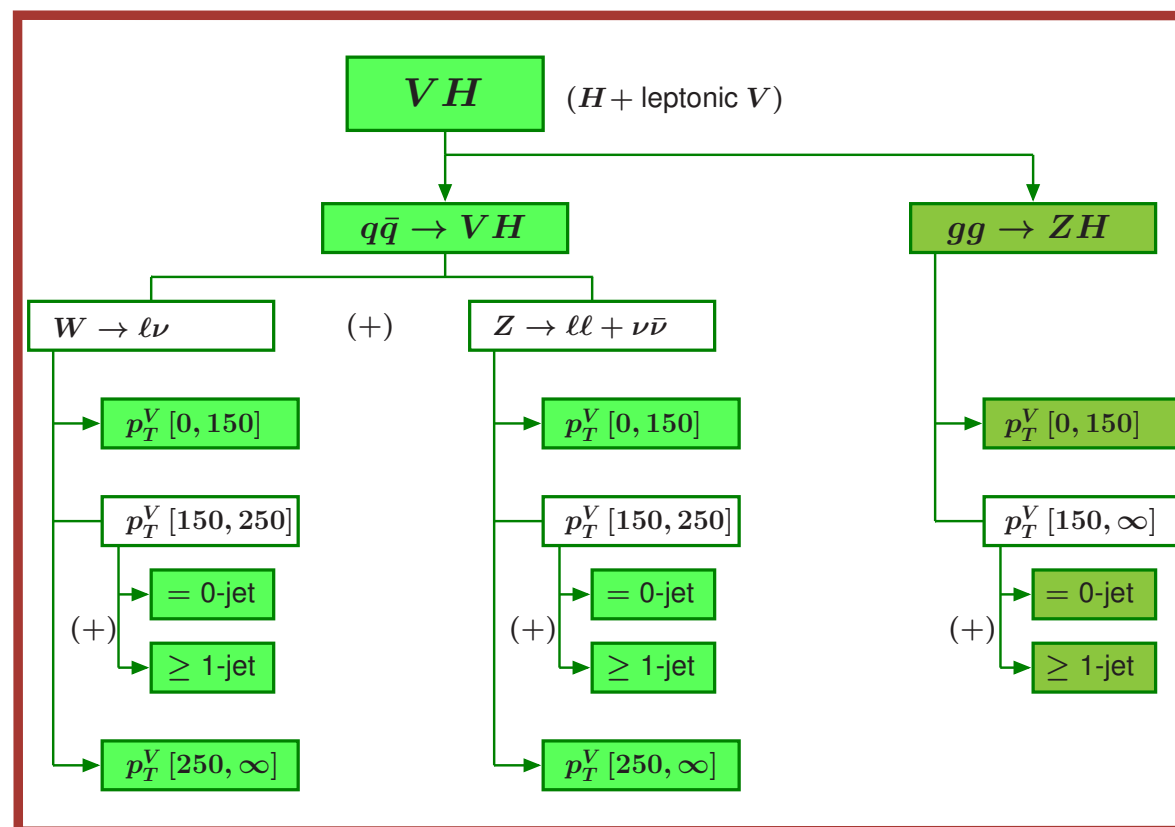
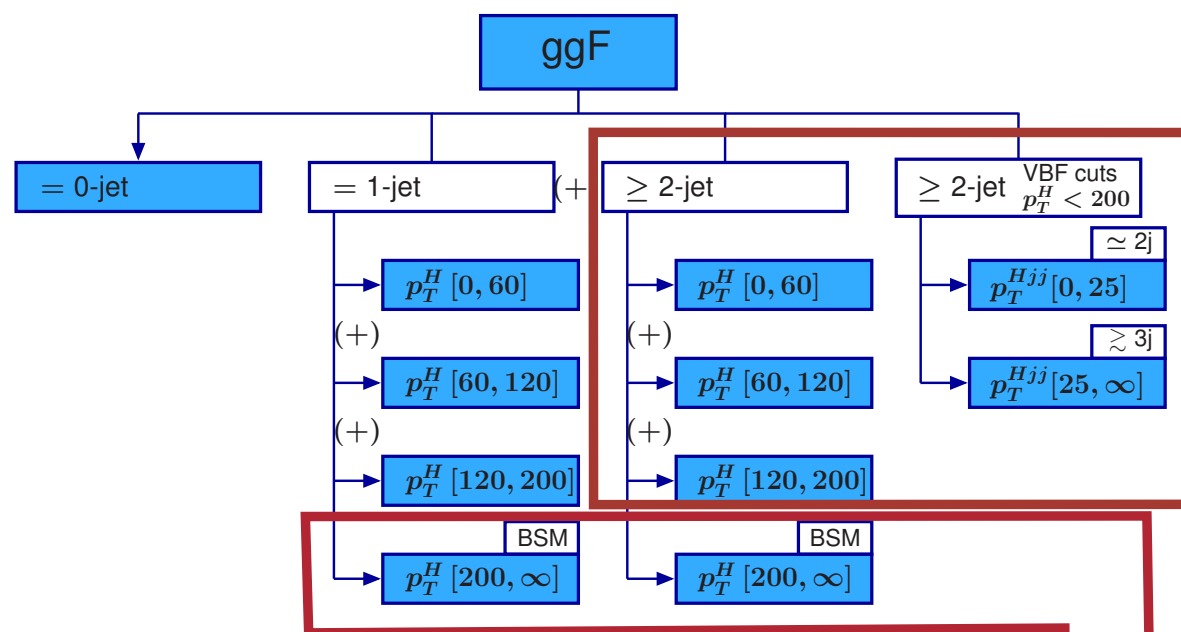
Simplified template cross sections (STXS) provide a natural evolution of signal strength measurements

Maximize sensitivity of the measurements and reduce the theory dependences that get directly folded into measurements

STXS stage-1 regions ($|y_H| < 2.5$).

ATLAS preliminary

$$y_i = \sum_i A_{i,j} \cdot r_i \cdot (\sigma_i \cdot B_{4l})_{SM} \cdot r_f \cdot \left(\frac{B_f}{B_{4l}} \right) \cdot \mathcal{L}$$



Regions enclosed by **red boxes are merged**, **except** for those indicated by the "±" sign **bbH is merged** with the **ggF**

$gg \rightarrow H$ (0-jet)

$gg \rightarrow H$ (1-jet, $p_T^H < 60$ GeV)

$gg \rightarrow H$
(1-jet, $60 \leq p_T^H < 120$ GeV)

$gg \rightarrow H$
(1-jet, $120 \leq p_T^H < 200$ GeV)

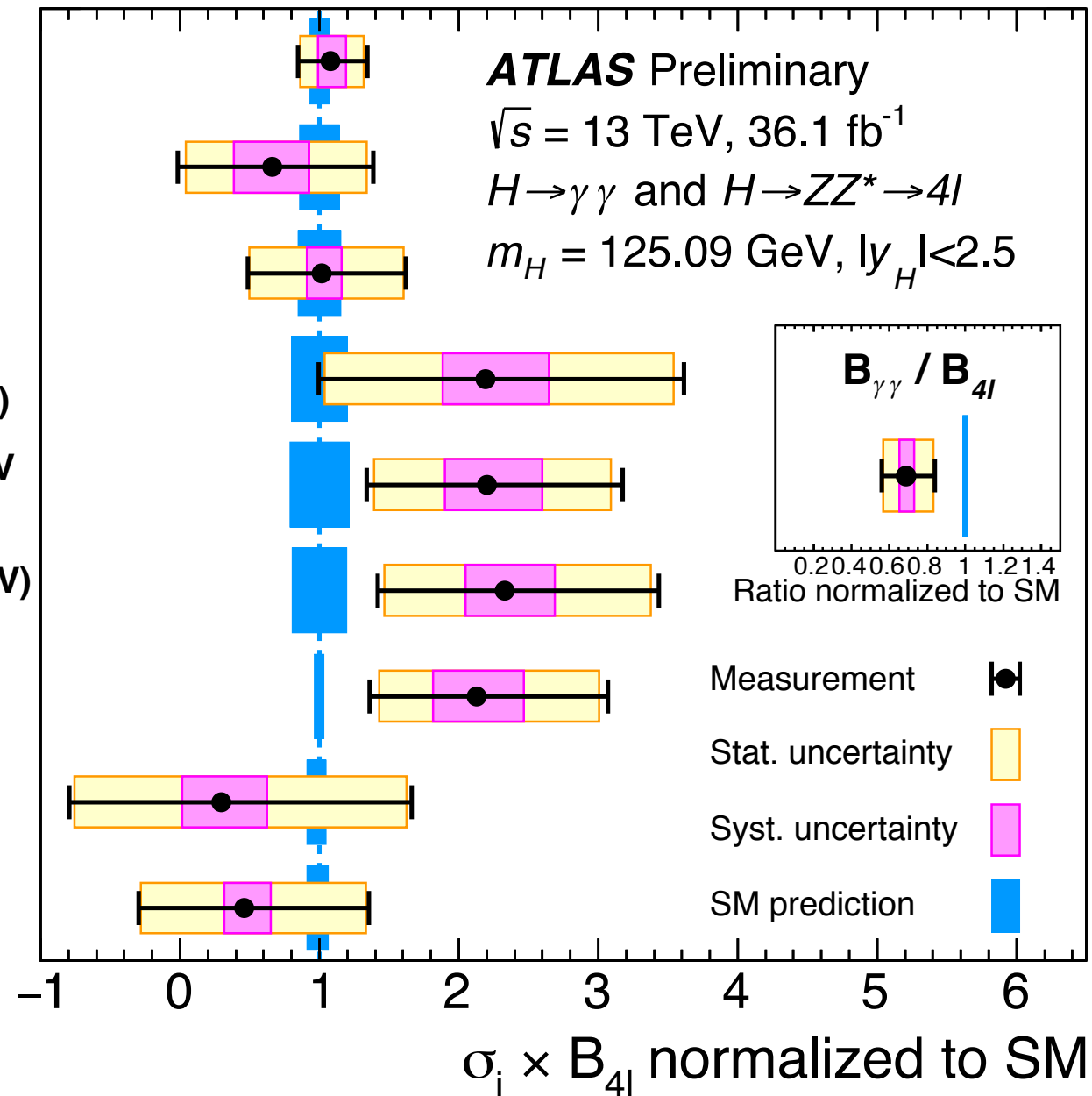
$gg \rightarrow H$ (≥ 2 -jet, $p_T^H < 200$ GeV
or VBF-like)

$gg \rightarrow H$ (≥ 1 -jet, $p_T^H \geq 200$ GeV)
+ $qq \rightarrow Hqq$ ($p_T^j \geq 200$ GeV)

$qq \rightarrow Hqq$ ($p_T^j < 200$ GeV)

$gg/qq \rightarrow Hll/Hl\nu$

$gg/qq \rightarrow ttH$



Results give a **good overall agreement with SM predictions** in a range of kinematic regions of Higgs boson production processes

The compatibility of the measurements with the SM expectation corresponds to a ***p-value of 9%***

$B_{\gamma\gamma} / B_{4l}$

$gg \rightarrow H$ (0-jet)

$gg \rightarrow H$ (1-jet, $p_T^H < 60$ GeV)

$gg \rightarrow H$
(1-jet, $60 \leq p_T^H < 120$ GeV)

$gg \rightarrow H$
(1-jet, $120 \leq p_T^H < 200$ GeV)

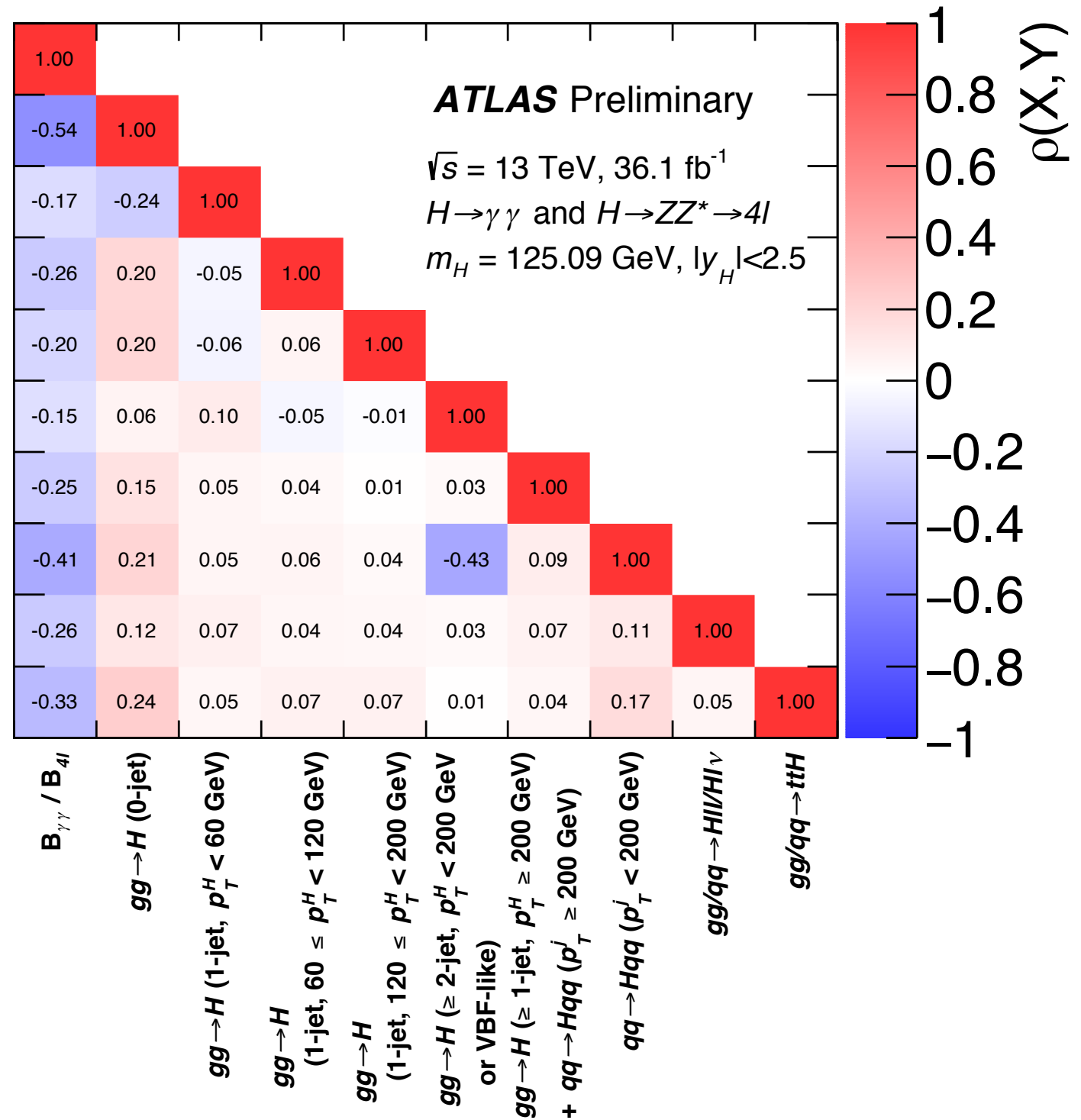
$gg \rightarrow H$ (≥ 2 -jet, $p_T^H < 200$ GeV
or VBF-like)

$gg \rightarrow H$ (≥ 1 -jet, $p_T^H \geq 200$ GeV)
+ $qq \rightarrow Hqq$ ($p_T^j \geq 200$ GeV)

$qq \rightarrow Hqq$ ($p_T^j < 200$ GeV)

$gg/qq \rightarrow Hll/Hl\nu$

$gg/qq \rightarrow ttH$



Correlations:

Largest between the BR ratio and $gg \rightarrow H$ 0-jet and $qq \rightarrow Hqq$ $p_T^j < 200$ GeV

$qq \rightarrow Hqq$ $p_T^j < 200$ GeV has greater tension between the two channels.

Significant between $gg \rightarrow H$ 0-jet and $gg \rightarrow H$ 1-jet $p_T^H < 60$ GeV, due to migrations between experimental jet-bin categories

$$\sigma(i \rightarrow H \rightarrow f) = \kappa_i^2 \sigma_i^{SM} \frac{\kappa_f^2 \Gamma_f^{SM}}{\kappa_H^2 \Gamma_H^{SM}}$$

- **Leading-order (LO) framework (limited predictive power)** developed by the LHC Higgs Cross Section WG to study Higgs couplings

useful as long as the overall picture is SM-like

- **Potential deviations from the SM predictions** of the Higgs boson couplings to SM bosons and fermions **encoded into** a set of **coupling modifiers**:

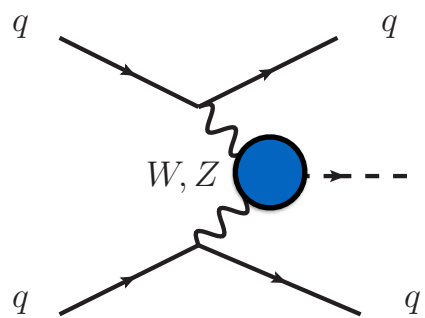
$$\kappa_i^2 = \frac{\sigma_i}{\sigma_i^{SM}} \quad \kappa_f^2 = \frac{B_f}{B_f^{SM}} \quad \kappa_H^2 = \sum_j B_j^{SM} \kappa_j^2 \quad \Gamma_H = \frac{\kappa_H^2 \Gamma_H^{SM}}{1 - B_{BSM}}$$

production

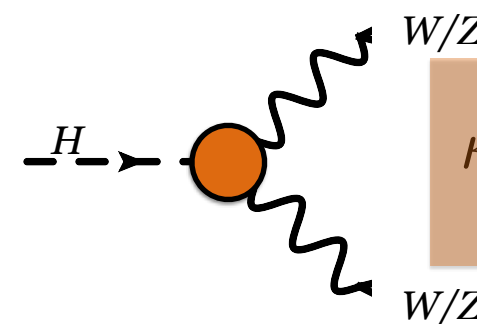
decay

Total width

- The **same couplings** are **involved in production and decay modes**, hence the yield measurements need to be projected onto the individual couplings



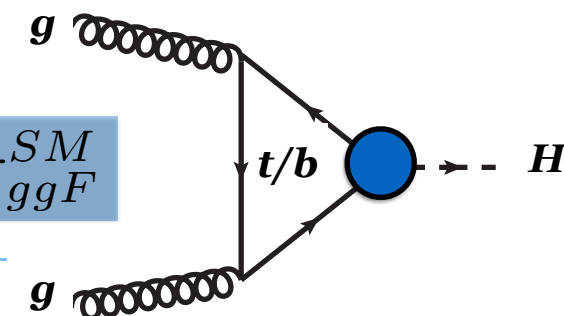
$$\sigma_{VBF} = (0.74 \cdot \kappa_W^2 + 0.26 \cdot \kappa_Z^2) \cdot \sigma_{VBF}^{SM}$$

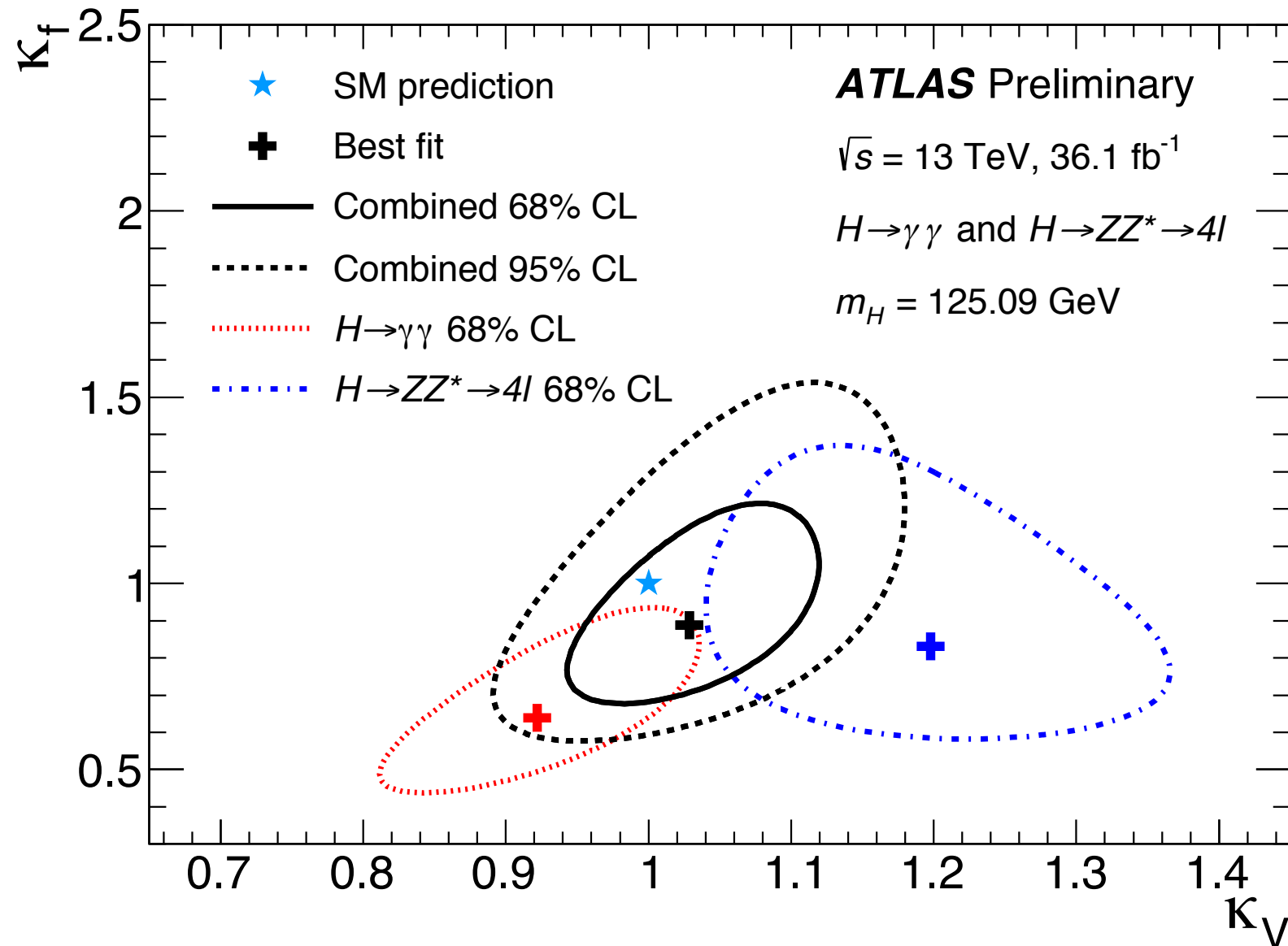


$$\kappa_{W,Z}^2 = \frac{\Gamma_{W,Z}}{\Gamma_{W,Z}^{SM}}$$

- Loops ($ggF, H \rightarrow \gamma\gamma$) either expressed with **effective coupling modifiers** κ_g, κ_γ , or using more **fundamental coupling modifiers** κ_x

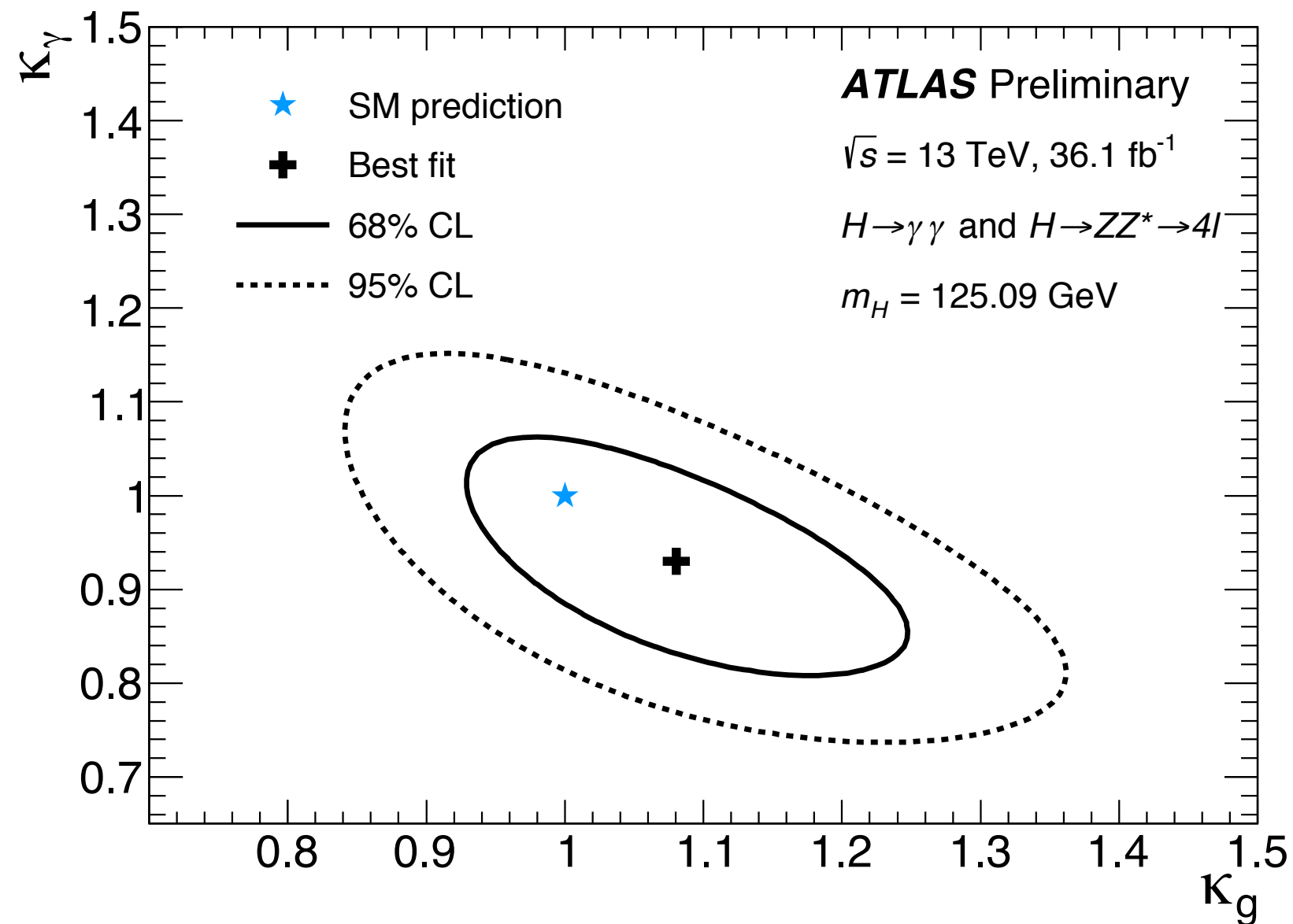
$$\sigma_{ggF} = \kappa_g \cdot \sigma_{ggF}^{SM} = (1.06 \cdot \kappa_t^2 + 0.01 \cdot \kappa_b^2 - 0.07 \cdot \kappa_t \kappa_b) \cdot \sigma_{ggF}^{SM}$$





Boson vs. fermion couplings

- SM Higgs couplings to fermions and boson very different (*Yukawa* vs $D\mu \rightarrow \kappa_F$ vs κ_V)
- κ_F, κ_V in agreement with SM
- $\kappa_F < 0$ excluded at $> 95\%$ CL
- 2D compatibility with SM: ***p-value* = 52%**



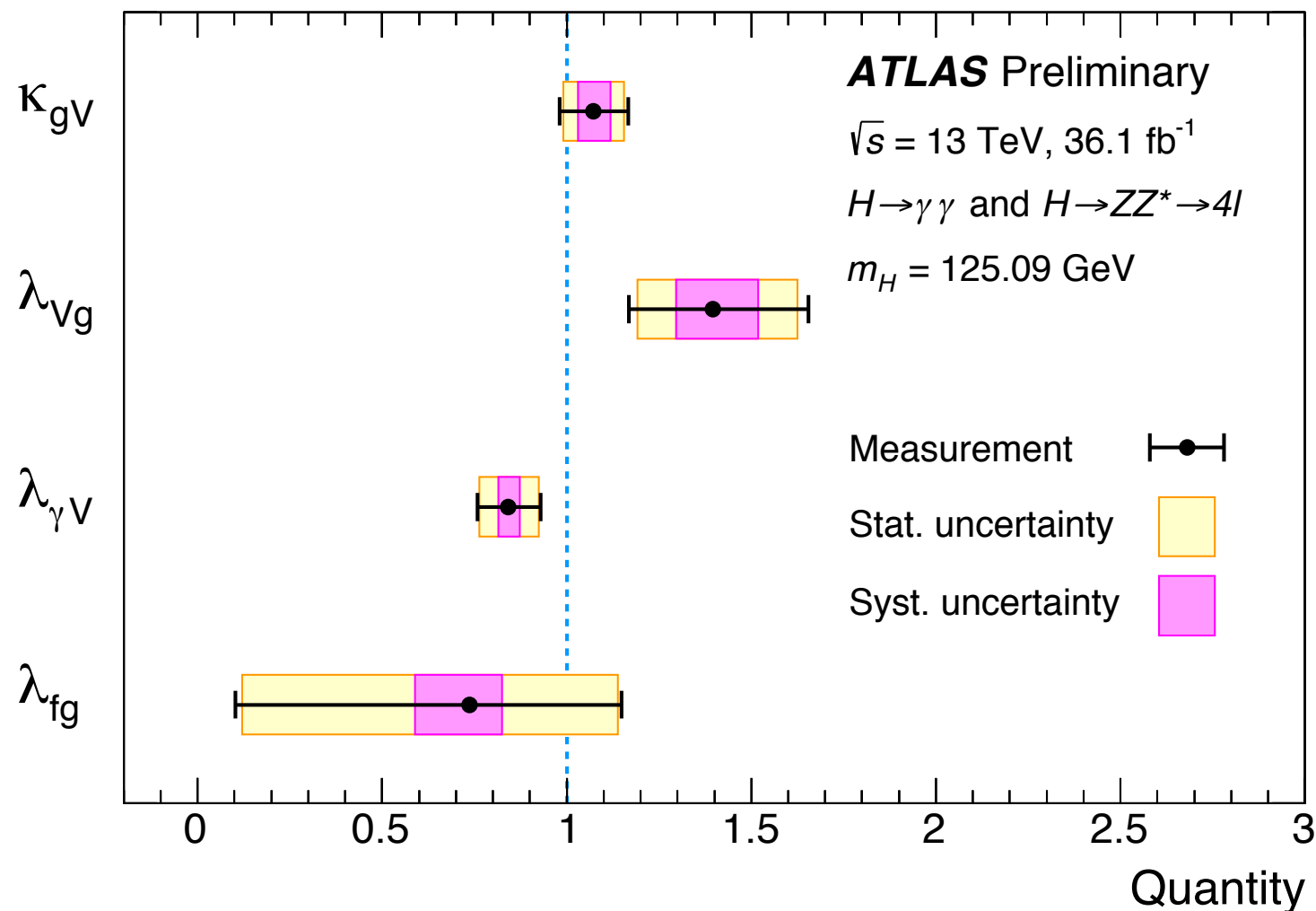
Effective couplings for κ_γ and κ_g

- No BSM decays (BBSM = 0)
- ***ggF*** and ***Hγγ*** loops are ***allowed to be affected by contributions from additional particles***
- ***2 free parameters κ_γ , κ_g*** , all other coupling modifiers fixed to their SM values
- 2D compatibility with SM: ***p-value = 68%***

Conversion of signal strength ratios to the κ -framework using: $\lambda_{ij} = \frac{\kappa_i}{\kappa_j}$

Four ratios constructed to probe loop vertices (κ_g, κ_γ), total width κ_H and fermion and vector couplings (κ_f, κ_V)

$$\kappa_{gV} = \frac{\kappa_g \kappa_V}{\kappa_H}, \quad \lambda_{Vg} = \frac{\kappa_V}{\kappa_g}, \quad \lambda_{fg} = \frac{\kappa_f}{\kappa_g}, \quad \lambda_{\gamma V} = \frac{\kappa_\gamma}{\kappa_V}$$



$$\Gamma_H = \frac{\kappa_H^2 \Gamma_H^{SM}}{1 - B_{BSM}}$$

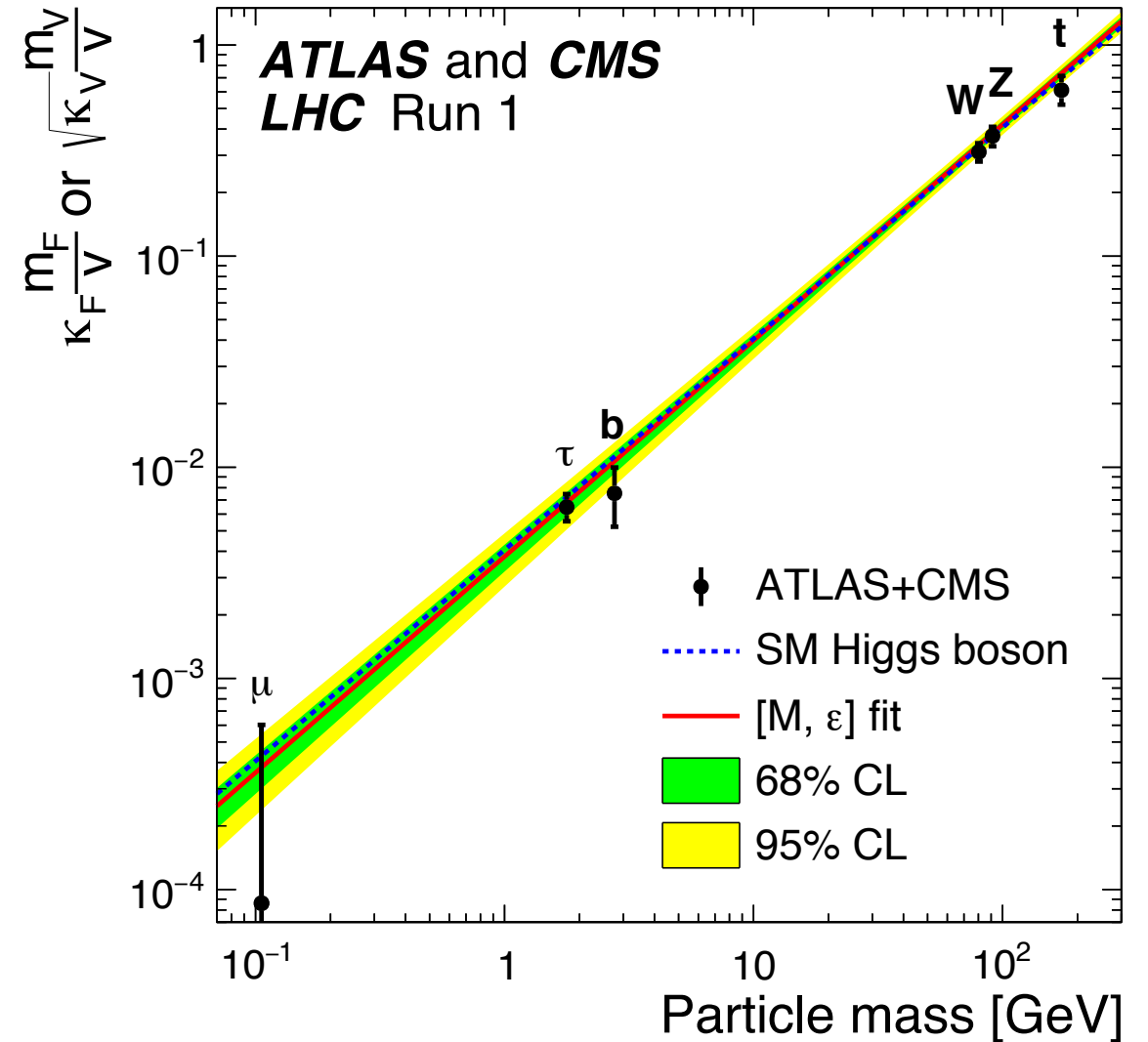
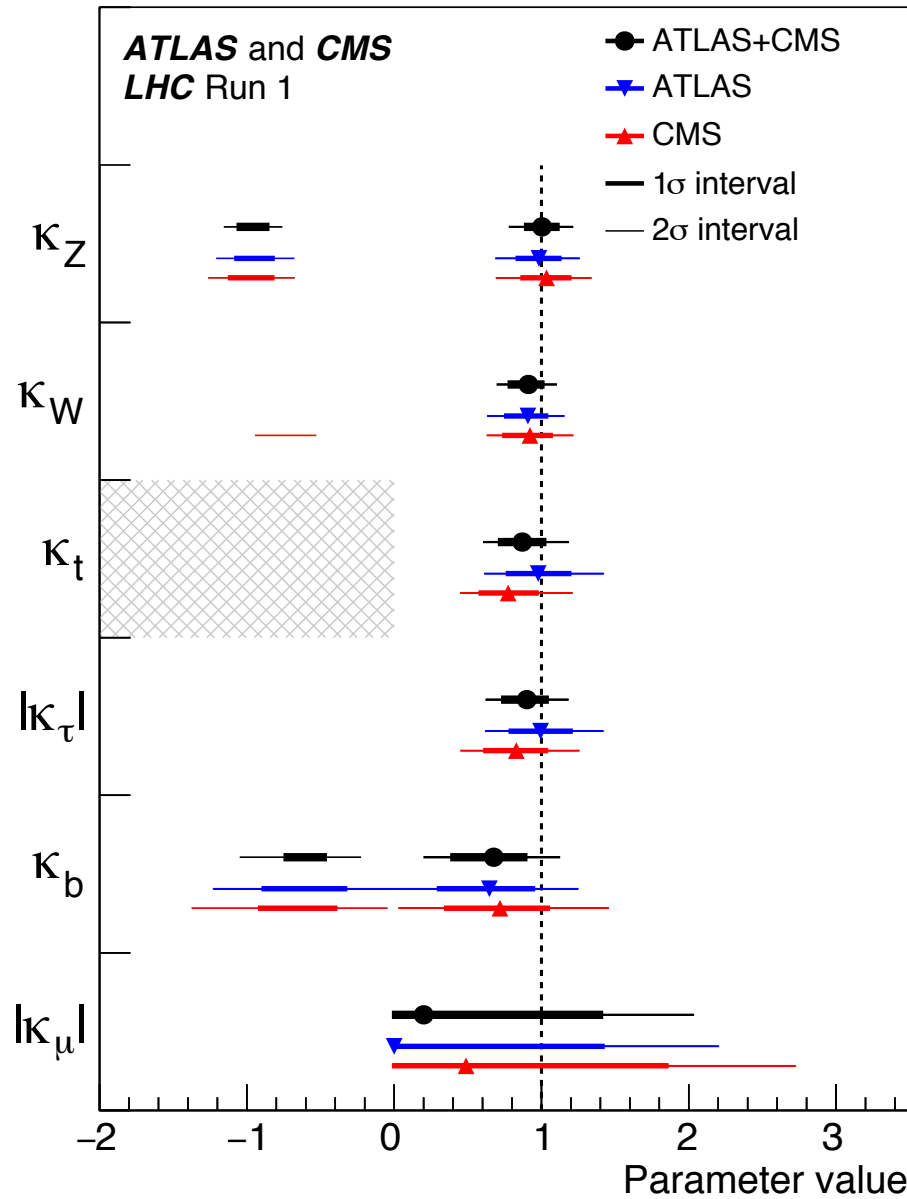
Negative ranges allowed for λ_{fg} to exploit the moderate sensitivity to the relative sign from tHX and $ggZH$

Best fit > 0 , but limited sensitivity to interference terms

4D compatibility with SM:
 p -value = 15%

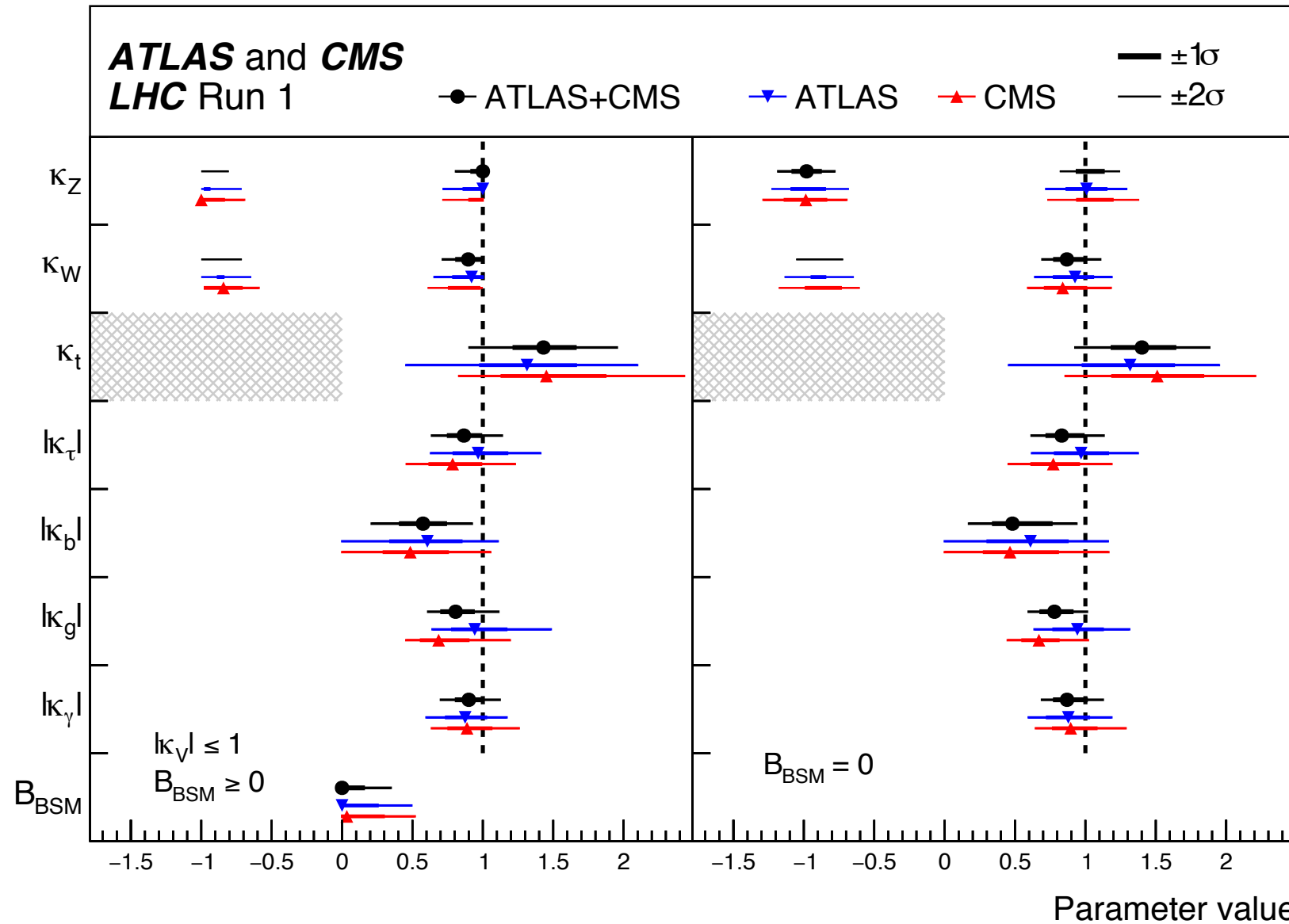
Express $\kappa_{g,H,\gamma}$ with other κ s, $BR_{BSM} = 0$, $H \rightarrow \mu\mu$ also combined

Coupling modifiers lower than those predicted by the SM when compared to the global signal strength or the fit results of the decay signal strengths



Parameterization derived from the coupling modifiers make the dependence on the particle masses explicit (as in the SM):

linear for the fermion Yukawa couplings and quadratic for the gauge couplings of the Higgs to the V-bosons



$$\Gamma_H = \frac{\kappa_H^2 \Gamma_H^{SM}}{1 - B_{BSM}}$$

- Probe new decay channels: **NWA**, $B_{BSM} > 0$ and impose $|\kappa_V| < 1$
- upper limit of $B_{BSM} = \mathbf{0.34}$ at **95% CL** (*expected limit: 0.39*)
- The ***p-value*** of the compatibility between the data and the SM predictions is **11%**, assuming that $B_{BSM} = 0$

Run-1 (ATLAS+CMS)

- Mass measured at 0.2% level : $m_H = 125.09 \pm 0.24 \text{ GeV}$
- Various parameterization explored and were all found in agreement with SM (worst p-value of 11%)

Run-2 (ATLAS: $H \rightarrow \gamma\gamma$ & $H \rightarrow 4l$)

- $m_H = 124.98 \pm 0.28 \text{ GeV}$, in agreement with ATLAS+CMS Run-1 result
- Preliminary combination results for coupling modifiers, production mode and total cross sections
- **Possible improvements over the kappa-framework being investigated: preliminary results shown from STXS framework, future considerations: EFT and PO**

All measurements consistent with SM expectations

- Run-1 ATLAS+CMS combination provides the most accurate measurements in the Higgs sector, though the ATLAS Run-2 combination approaching the same accuracy
- **Increased statistics from the final Run-II dataset and improved theory predictions are already providing a significant increase in sensitivity**

Higgs boson discovery:

- ATLAS: [Phys. Lett. B 716 \(2012\) 1-29](#)
- CMS: [Phys. Lett. B 716 \(2012\) 30](#)

ATLAS+CMS combination:

- Mass: [Phys. Rev. Lett. 114, \(2015\)](#)
- Couplings: [JHEP 08 \(2016\) 045](#)

ATLAS and CMS individual combinations:

- ATLAS: [Eur. Phys. J. C 76 \(2016\) 6](#)
- CMS: [Eur. Phys. J. C 75 \(2015\) 212](#)

ATLAS $H\gamma\gamma$ Mass shift through interferometry: [ATL-PHYS-PUB-2016-009](#)

13 TeV ATLAS $H\rightarrow\gamma\gamma$ & $H\rightarrow 4l$ combination:

- Mass: [ATLAS-CONF-2017-046](#)
- XS & couplings: [ATLAS-CONF-2017-047](#)

13 TeV ATLAS combination inputs:

- $H\rightarrow\gamma\gamma$: [ATLAS-CONF-2017-045](#)
- $H\rightarrow 4l$: [ATLAS-CONF-2017-043](#)

ATLAS+CMS combination inputs:

$H\rightarrow\gamma\gamma$

- ATLAS: [Phys. Rev. D 90, 112015 \(2014\)](#)
- CMS: [EPJC 10.2014, 74:3076](#)

$H\rightarrow ZZ$

- ATLAS: [Phys. Rev. D 91, 012006 \(2015\)](#)
- CMS: [Phys. Rev. D 89, 092007](#)

$H\rightarrow WW$

- ATLAS [Phys. Rev. D 92, 012006 \(2015\)](#),
[JHEP 08.2015, 2015:137](#)
- CMS: [JHEP 01.2014, 2014:96](#)

$H\rightarrow\tau\tau$

- ATLAS: [JHEP April 2015, 2015:117](#)
- CMS: [JHEP 05 \(2014\) 104](#)

$H\rightarrow bb$

- ATLAS: [JHEP 01.2015, 2015:69](#)
- CMS: [Phys. Rev. D 89 01.2014](#)

$H\rightarrow\mu\mu$

- ATLAS: [Physics Letters B 738 \(2014\) 68-86](#)
- CMS: [Physics Letters B V\(744\), 11.05.2015](#)

ttH

- ATLAS: [Eur. Phys. J. C \(2015\) 75:349](#),
[Phys. Letters B 749 \(2015\) 519-541](#)
- CMS: [JHEP 05.2013, 2013:145](#), [JHEP 09 \(2014\) 087](#)

Additional material

Combine categories and **fit** for **cross sections** (σ_i) or **signal strength** of different **production processes** (i) and **final states** (f)

$$\mu_i = \frac{\sigma_i}{\sigma_{i,SM}} \quad \mu^f = \frac{B^f}{B_{SM}^f} \quad \mu_i^f = \frac{\sigma_i \cdot B^f}{(\sigma_i \cdot B^f)_{SM}}$$

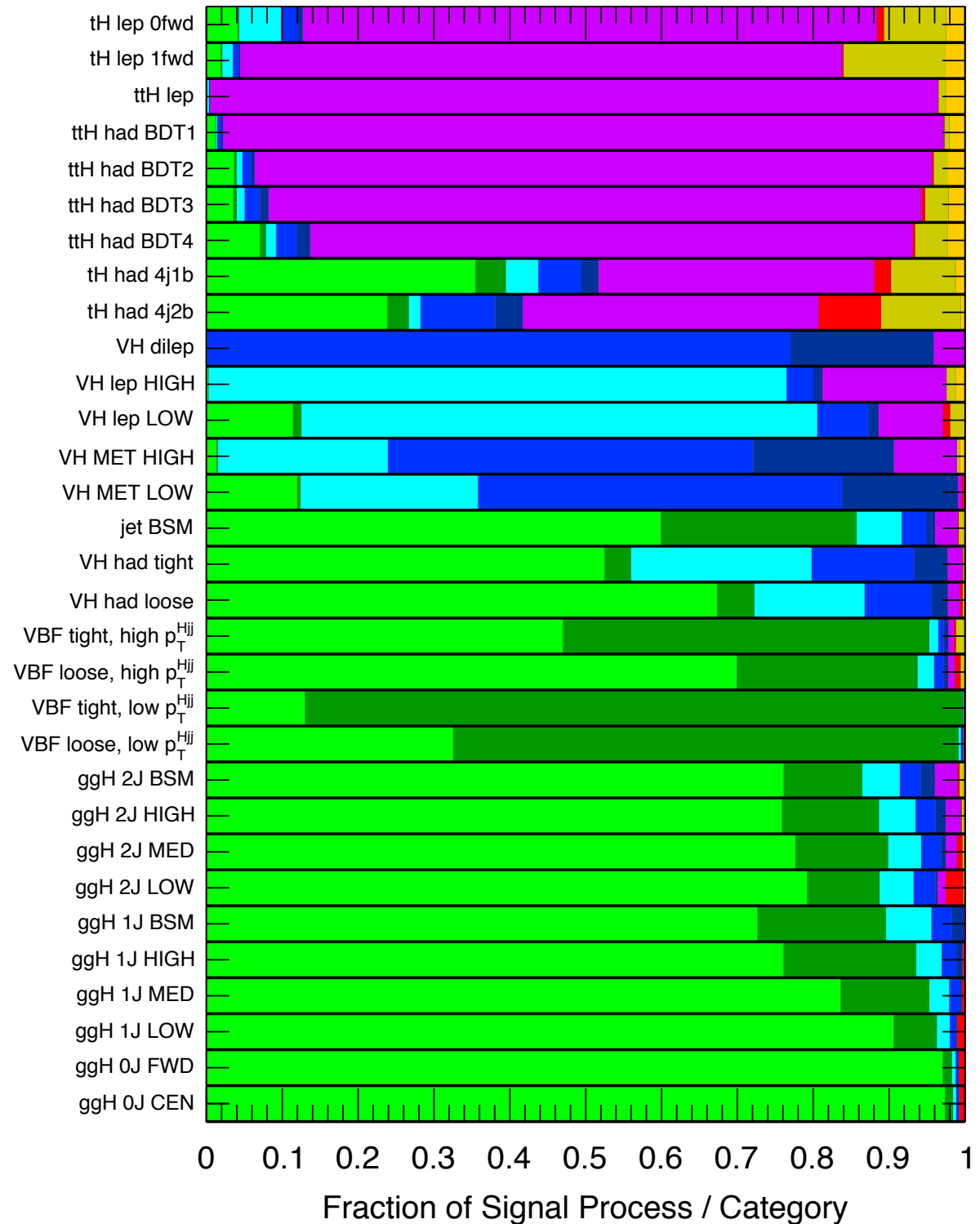
Analyses extract signal yields:

$$\begin{aligned} \nu^{\text{sig}} &= \mathcal{L} \sum_i \sum_f \left(\sigma_i A_{i,SM}^f \epsilon_{i,SM}^f B^f \right) \\ &= \mathcal{L} \sum_i \sum_f \left(\mu_i \sigma_{i,SM} A_{i,SM}^f \epsilon_{i,SM}^f \mu^f B_{SM}^f \right) \end{aligned}$$

where \mathcal{L} is the luminosity, ϵ efficiencies, A the detector acceptance and μ_i, μ^f are production and decay signal strengths

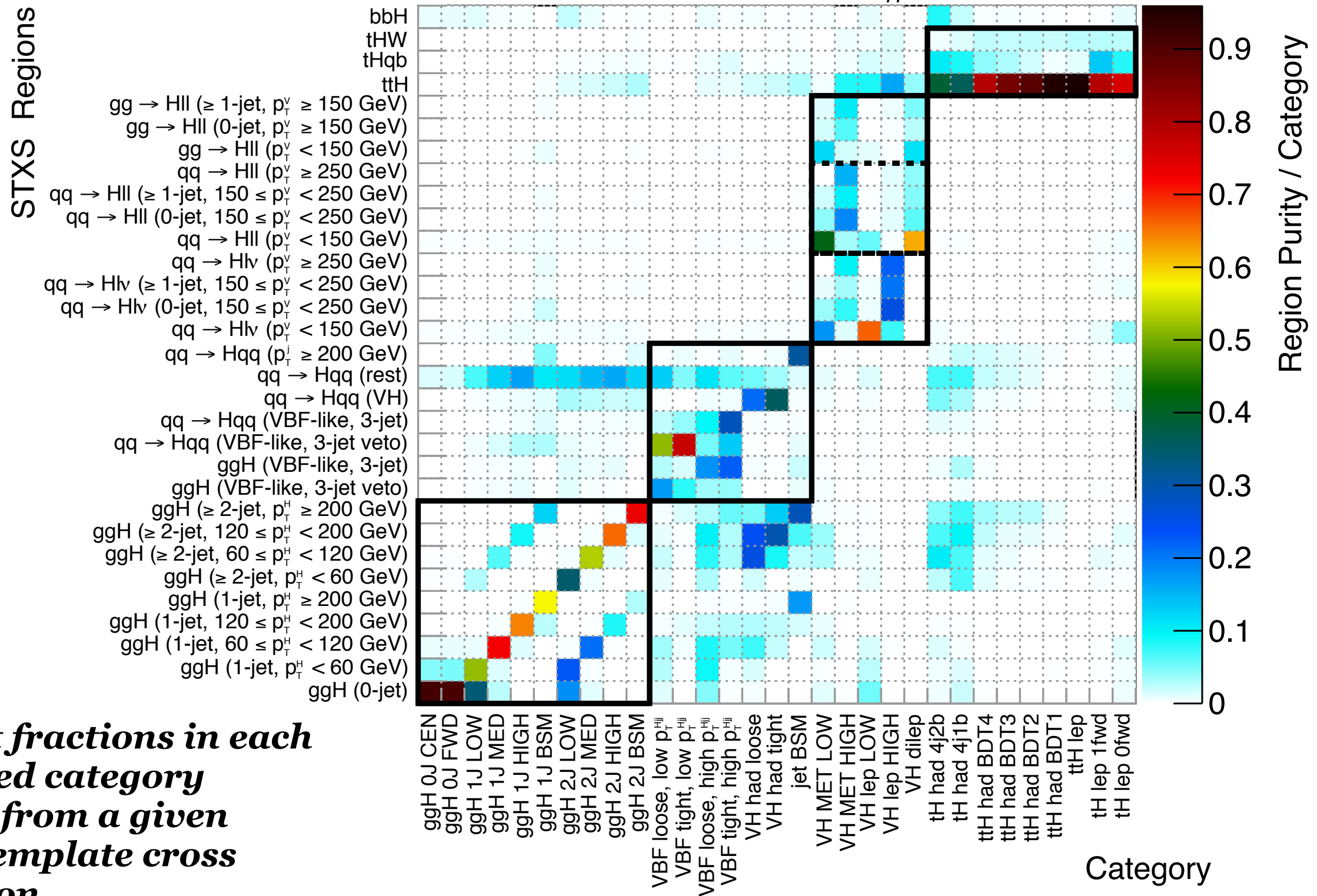


ATLAS Preliminary $H \rightarrow \gamma\gamma$, $m_H = 125.09$ GeV



The expected composition of the selected Higgs boson events, in terms of the different production modes, for each reconstructed category

ATLAS Preliminary $H \rightarrow \gamma\gamma, m_H = 125.09$ GeV



signal event fractions in each reconstructed category originating from a given simplified template cross section region

$H \rightarrow \gamma\gamma$

$t\bar{t}H+tH$ leptonic (two tHX and one $t\bar{t}H$ categories)

$t\bar{t}H+tH$ hadronic (two tHX and four BDT $t\bar{t}H$ categories)

VH dilepton

VH one-lepton, $p_T^{\ell+\text{MET}} \geq 150 \text{ GeV}$

VH one-lepton, $p_T^{\ell+\text{MET}} \text{ ; } 150 \text{ GeV}$

VH $E_T^{\text{miss}}, E_T^{\text{miss}} \geq 150 \text{ GeV}$

VH $E_T^{\text{miss}}, E_T^{\text{miss}} \text{ ; } 150 \text{ GeV}$

$VH+VBF$ $p_T^{j1} \geq 200 \text{ GeV}$

VH hadronic (BDT tight and loose categories)

VBF, $p_T^{\gamma\gamma jj} \geq 25 \text{ GeV}$ (BDT tight and loose categories)

VBF, $p_T^{\gamma\gamma jj} \text{ ; } 25 \text{ GeV}$ (BDT tight and loose categories)

ggF 2-jet, $p_T^{\gamma\gamma} \geq 200 \text{ GeV}$

ggF 2-jet, $120 \text{ GeV} \leq p_T^{\gamma\gamma} \text{ ; } 200 \text{ GeV}$

ggF 2-jet, $60 \text{ GeV} \leq p_T^{\gamma\gamma} \text{ ; } 120 \text{ GeV}$

ggF 2-jet, $p_T^{\gamma\gamma} < 60 \text{ GeV}$

ggF 1-jet, $p_T^{\gamma\gamma} \geq 200 \text{ GeV}$

ggF 1-jet, $120 \text{ GeV} \leq p_T^{\gamma\gamma} \text{ ; } 200 \text{ GeV}$

ggF 1-jet, $60 \text{ GeV} \leq p_T^{\gamma\gamma} \text{ ; } 120 \text{ GeV}$

ggF 1-jet, $p_T^{\gamma\gamma} \text{ ; } 60 \text{ GeV}$

ggF 0-jet (central and forward categories)

$H \rightarrow ZZ^* \rightarrow 4\ell$

$t\bar{t}H$

VH leptonic

2-jet VH

2-jet VBF, $p_T^{j1} \geq 200 \text{ GeV}$

2-jet VBF, $p_T^{j1} \text{ ; } 200 \text{ GeV}$

1-jet ggF, $p_T^{4\ell} \geq 120 \text{ GeV}$

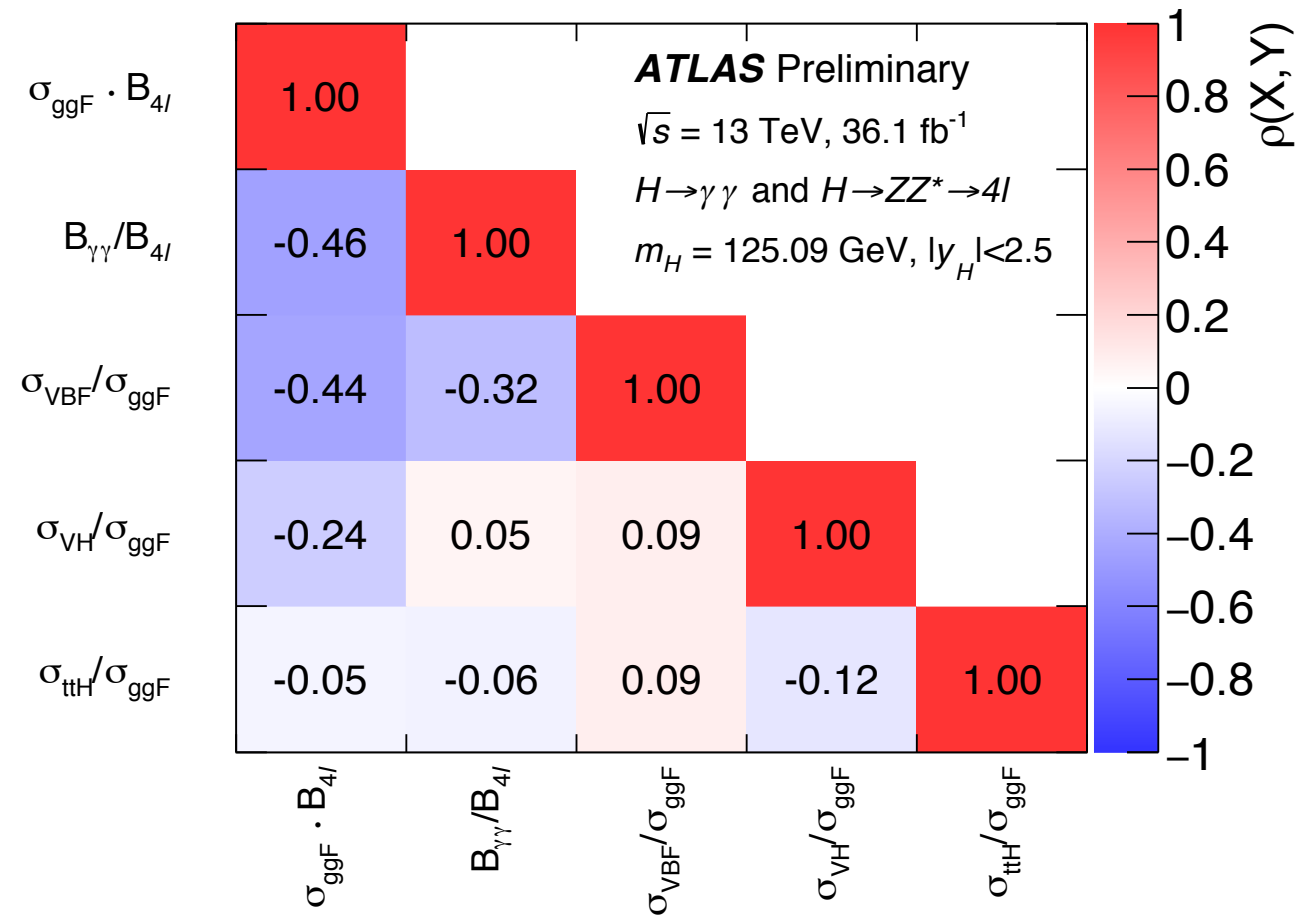
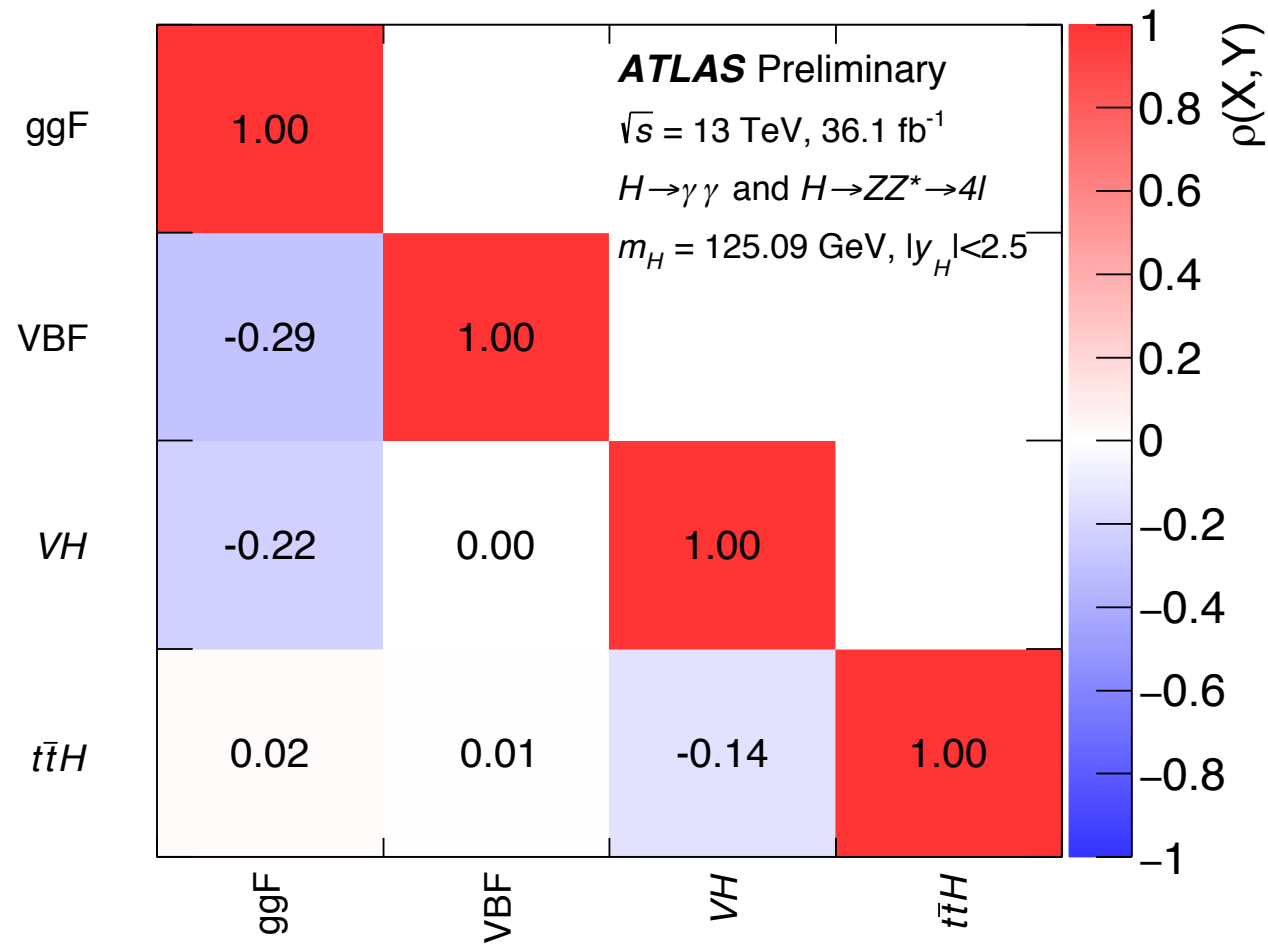
1-jet ggF, $60 \text{ GeV} \text{ ; } p_T^{4\ell} \text{ ; } 120 \text{ GeV}$

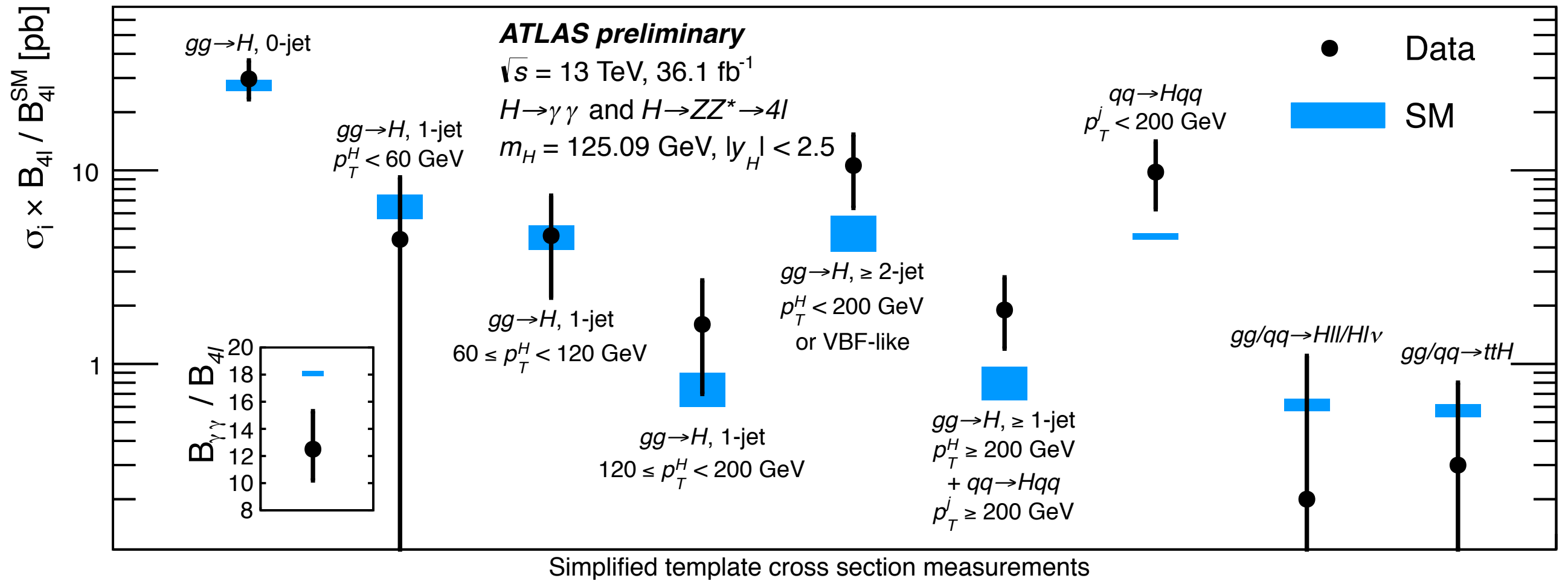
1-jet ggF, $p_T^{4\ell} \text{ ; } 60 \text{ GeV}$

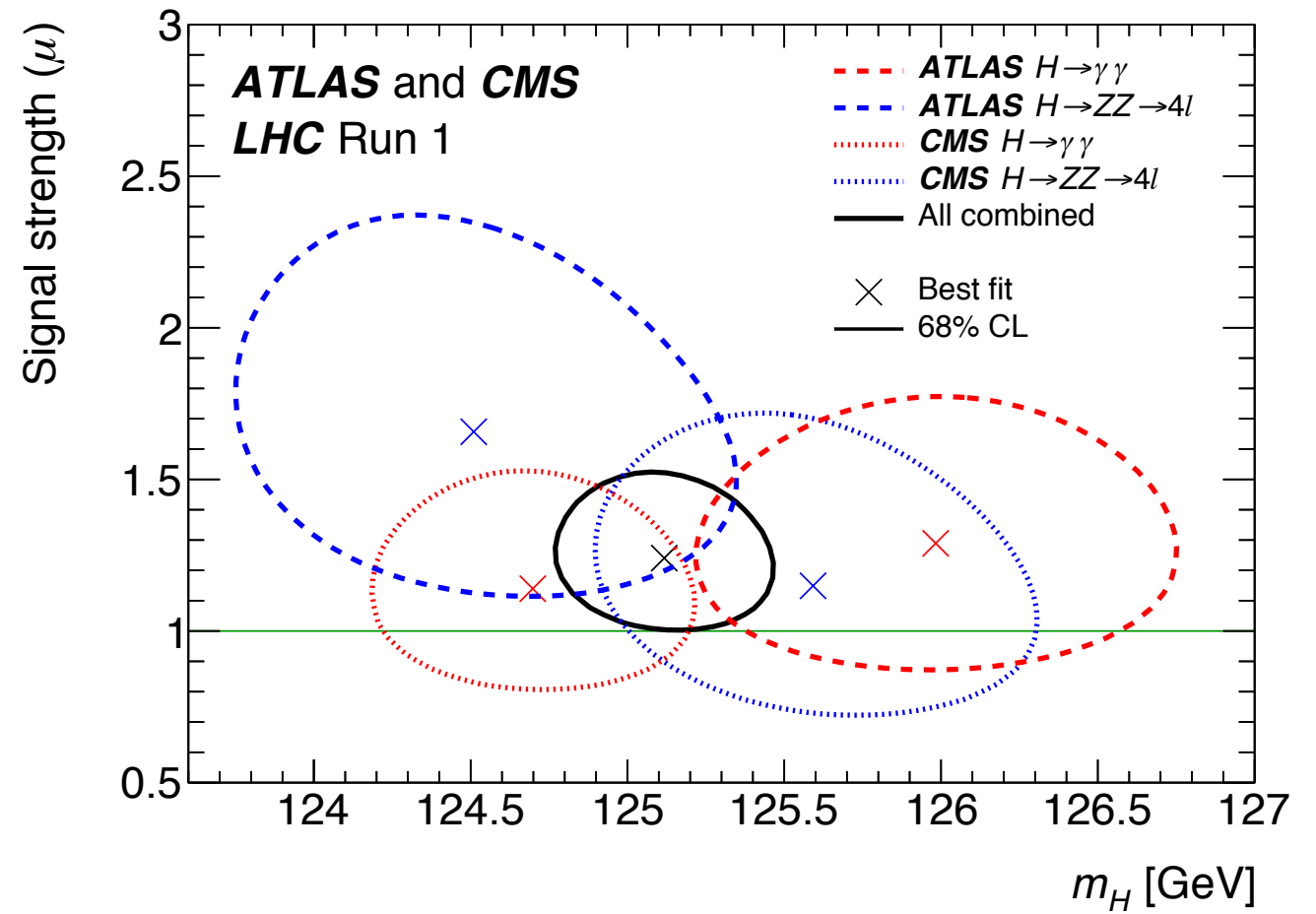
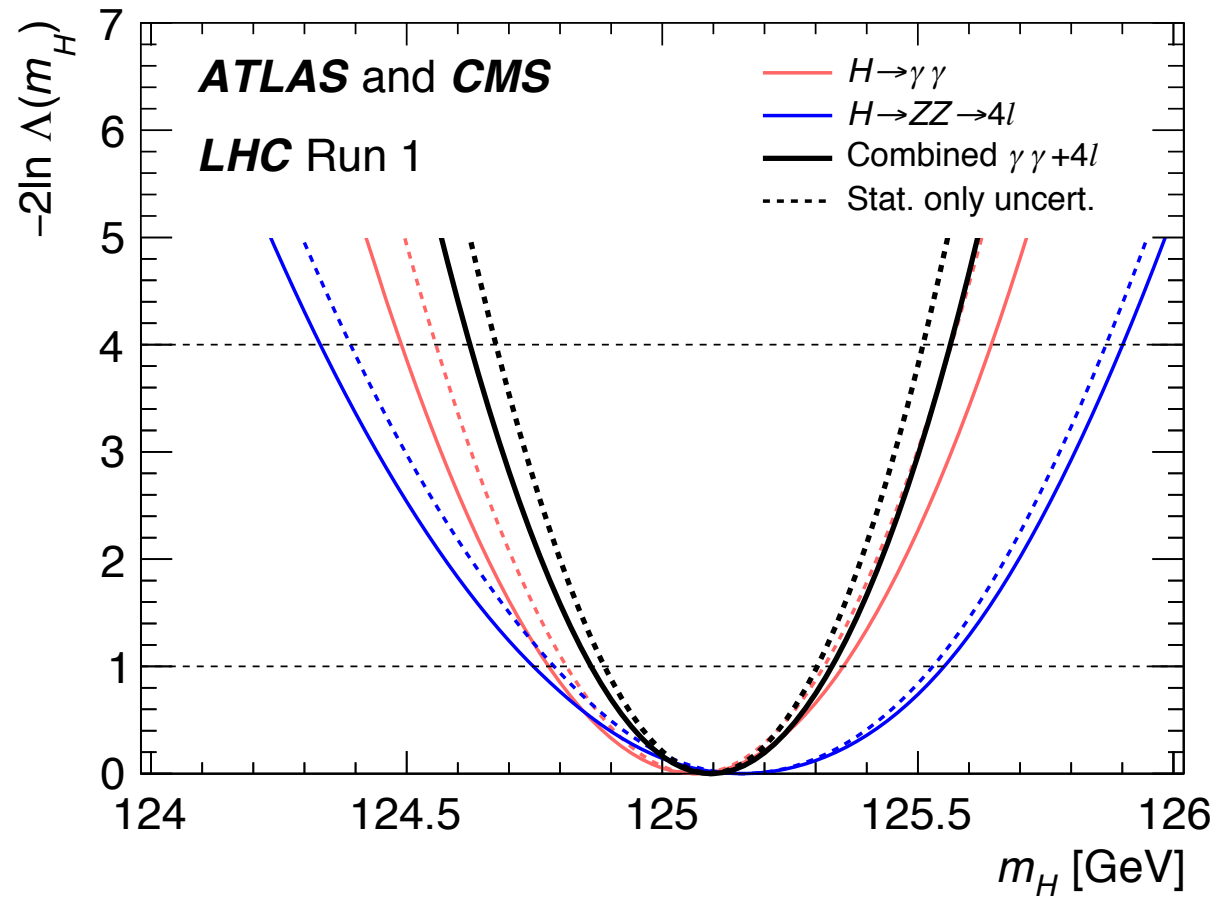
0-jet ggF

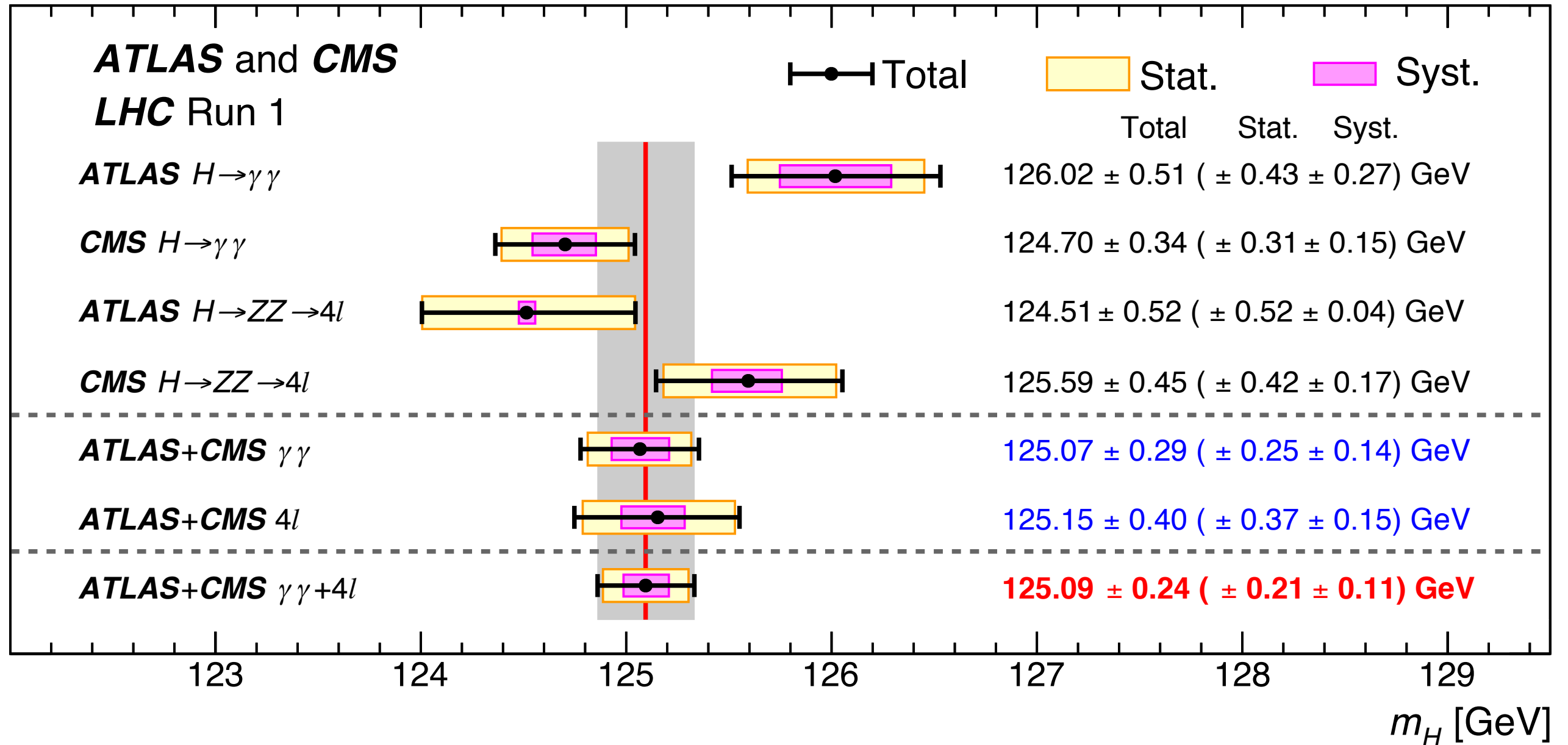
Stage 0 process	Measurement region	Stage 1 region
$gg \rightarrow H$	0-jet	0-jet
	1-jet, $p_T^H < 60 \text{ GeV}$	1-jet, $p_T^H < 60 \text{ GeV}$
	1-jet, $60 \leq p_T^H < 120 \text{ GeV}$	1-jet, $60 \leq p_T^H < 120 \text{ GeV}$
	1-jet, $120 \leq p_T^H < 200 \text{ GeV}$	1-jet, $120 \leq p_T^H < 200 \text{ GeV}$
	≥ 1 -jet, $p_T^H > 200 \text{ GeV}$	1-jet, $p_T^H > 200 \text{ GeV}$
		≥ 2 -jet, $p_T^H > 200 \text{ GeV}$
	≥ 2 -jet, $p_T^H < 200 \text{ GeV}$ or VBF-like	≥ 2 -jet, $p_T^H < 60 \text{ GeV}$
		≥ 2 -jet, $60 \leq p_T^H < 120 \text{ GeV}$
		≥ 2 -jet, $120 \leq p_T^H < 200 \text{ GeV}$
		VBF-like, $p_T^{Hjj} < 25 \text{ GeV}$
	VBF-like, $p_T^{Hjj} \geq 25 \text{ GeV}$	
$qq \rightarrow Hqq$	$p_T^j \geq 200 \text{ GeV}$	$p_T^j \geq 200 \text{ GeV}$
	$p_T^j < 200 \text{ GeV}$	$p_T^j < 200 \text{ GeV}$, VBF-like, $p_T^{Hjj} < 25 \text{ GeV}$
		$p_T^j < 200 \text{ GeV}$, VBF-like, $p_T^{Hjj} \geq 25 \text{ GeV}$
		$p_T^j < 200 \text{ GeV}$, VH-like
		$p_T^j < 200 \text{ GeV}$, Rest

ATLAS Run-2 cross section correlations.









Results from the **Run-1 ATLAS+CMS mass combination:**

Systematic uncertainty breakdown given in backup

Dominant uncertainties:

non-linearity, material in front of ECAL, muon calibration

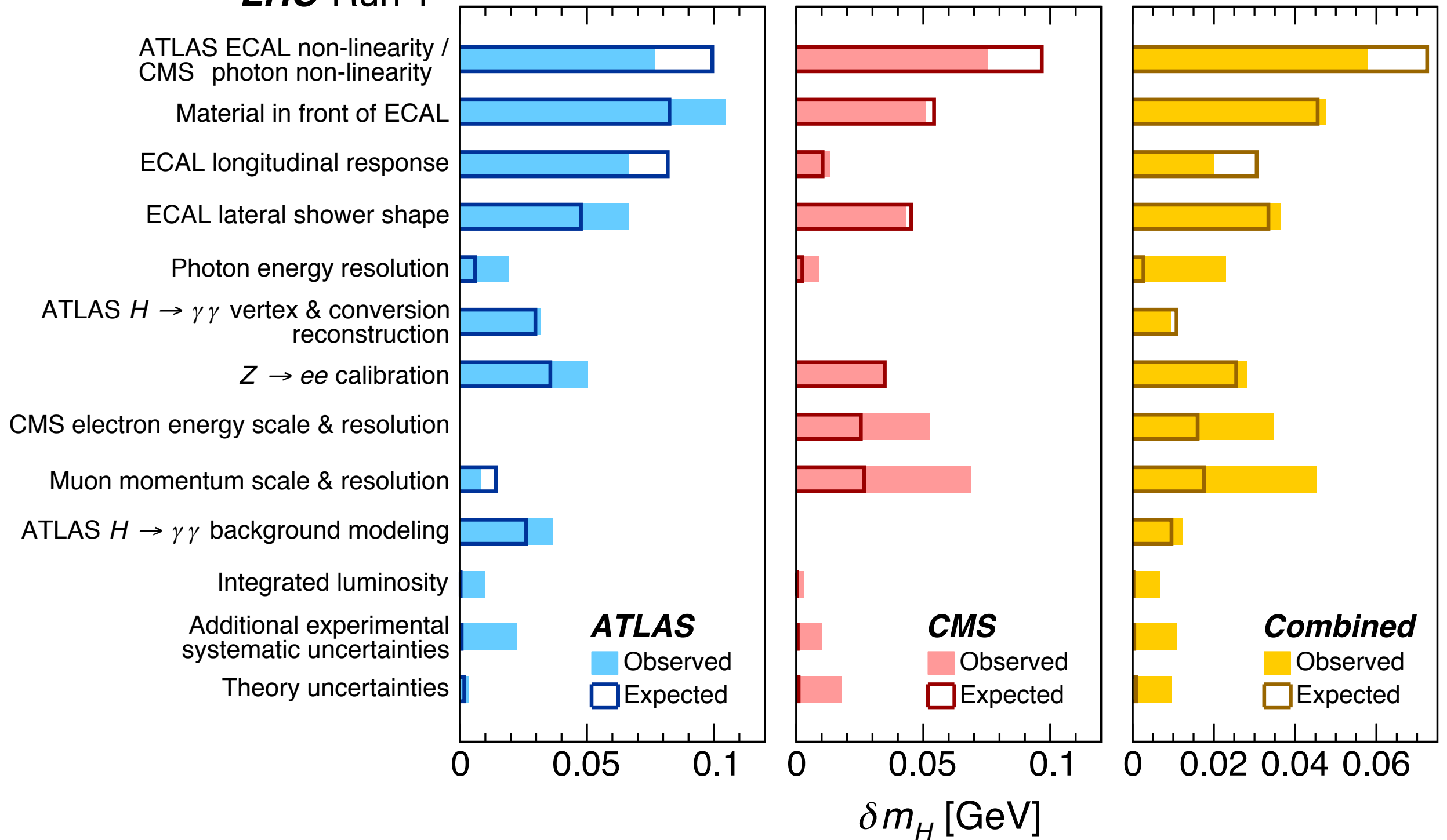
Mass systematic uncertainties.

ATLAS and CMS LHC Run 1

Uncertainty in ATLAS
combined result

Uncertainty in CMS
combined result

Uncertainty in LHC
combined result

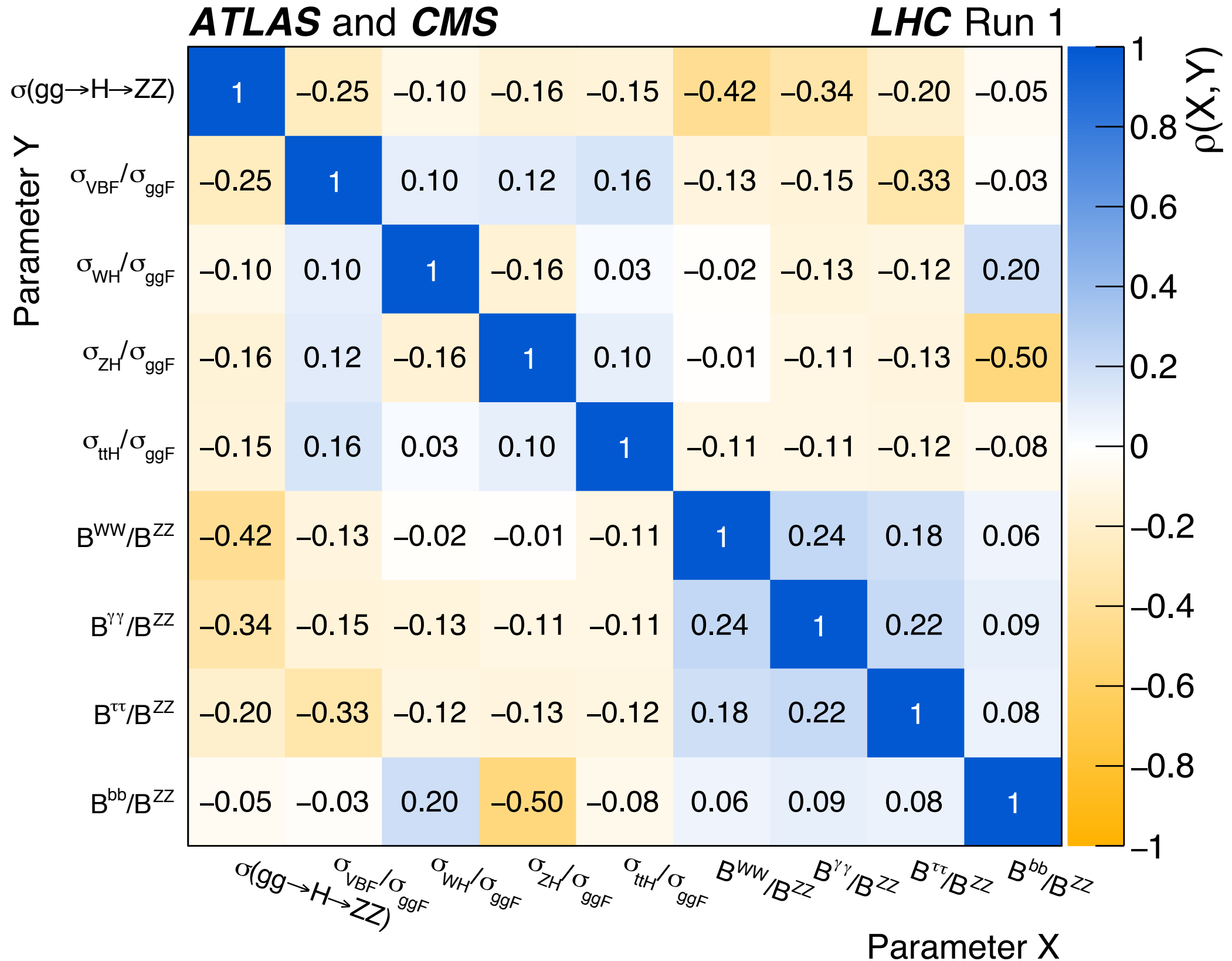


Couplings: compatibility with SM.

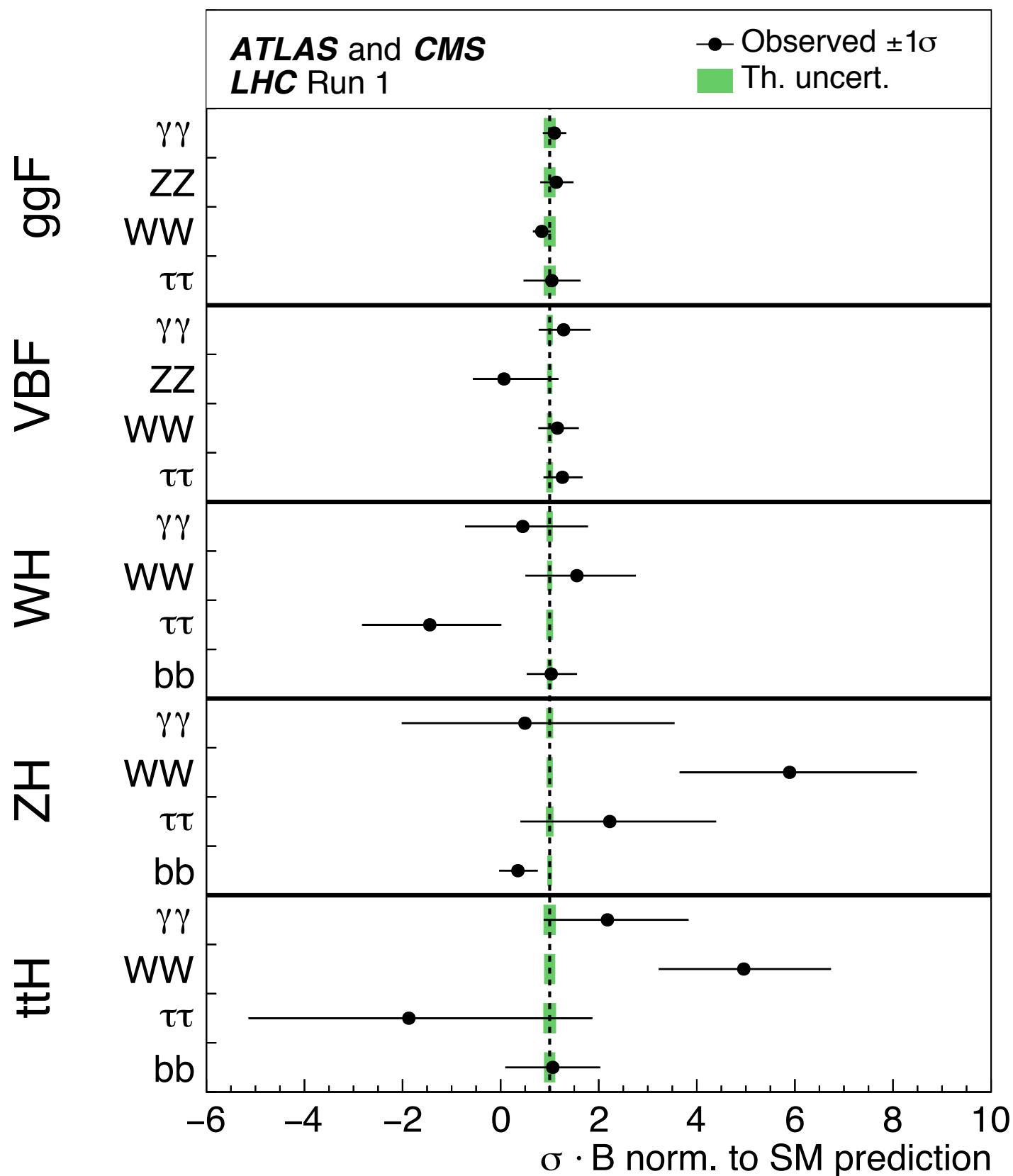
Parameterisation	p -value	DOF	Parameters
Global signal strength	40%	1	μ
Production processes	24%	5	$\mu_{ggF}, \mu_{VBF}, \mu_{WH}, \mu_{ZH}, \mu_{ttH}$
Decay modes	65%	5	$\mu^{\gamma\gamma}, \mu^{ZZ}, \mu^{WW}, \mu^{\tau\tau}, \mu^{bb}$
Decay modes with $H \rightarrow \mu\mu$	75%	6	$\mu^{\gamma\gamma}, \mu^{ZZ}, \mu^{WW}, \mu^{\tau\tau}, \mu^{bb}, \mu^{\mu\mu}$
μ_V and μ_F per decay	90%	10	$\mu_V^{\gamma\gamma}, \mu_V^{ZZ}, \mu_V^{WW}, \mu_V^{\tau\tau}, \mu_V^{bb}, \mu_F^{\gamma\gamma}, \mu_F^{ZZ}, \mu_F^{WW}, \mu_F^{\tau\tau}, \mu_F^{bb}$
μ_V / μ_F ratio	75%	6	$\mu_V / \mu_F, \mu_F^{\gamma\gamma}, \mu_F^{ZZ}, \mu_F^{WW}, \mu_F^{\tau\tau}, \mu_F^{bb}$
$\sigma_i \cdot B^f$ product	20%	23	$(\sigma \cdot B)_{ggF}^{\gamma\gamma}, (\sigma \cdot B)_{ggF}^{ZZ}, (\sigma \cdot B)_{ggF}^{WW}, (\sigma \cdot B)_{ggF}^{\tau\tau}, (\sigma \cdot B)_{VBF}^{\gamma\gamma}, (\sigma \cdot B)_{VBF}^{ZZ}, (\sigma \cdot B)_{VBF}^{WW}, (\sigma \cdot B)_{VBF}^{\tau\tau}, (\sigma \cdot B)_{WH}^{\gamma\gamma}, (\sigma \cdot B)_{WH}^{ZZ}, (\sigma \cdot B)_{WH}^{WW}, (\sigma \cdot B)_{WH}^{\tau\tau}, (\sigma \cdot B)_{WH}^{bb}, (\sigma \cdot B)_{ZH}^{\gamma\gamma}, (\sigma \cdot B)_{ZH}^{ZZ}, (\sigma \cdot B)_{ZH}^{WW}, (\sigma \cdot B)_{ZH}^{\tau\tau}, (\sigma \cdot B)_{ZH}^{bb}, (\sigma \cdot B)_{ttH}^{\gamma\gamma}, (\sigma \cdot B)_{ttH}^{ZZ}, (\sigma \cdot B)_{ttH}^{WW}, (\sigma \cdot B)_{ttH}^{\tau\tau}, (\sigma \cdot B)_{ttH}^{bb}$
Ratios of σ and BR relative to $\sigma(gg \rightarrow H \rightarrow ZZ)$	16%	9	$\sigma(gg \rightarrow H \rightarrow ZZ), \sigma_{VBF} / \sigma_{ggF}, \sigma_{WH} / \sigma_{ggF}, \sigma_{ZH} / \sigma_{ggF}, \sigma_{ttH} / \sigma_{ggF}, B^{WW} / B^{ZZ}, B^{\gamma\gamma} / B^{ZZ}, B^{\tau\tau} / B^{ZZ}, B^{bb} / B^{ZZ}$
Ratios of σ and BR relative to $\sigma(gg \rightarrow H \rightarrow ZZ)$ and 7/8 TeV	26%	14	$\sigma(gg \rightarrow H \rightarrow ZZ), \sigma_{VBF} / \sigma_{ggF}, \sigma_{WH} / \sigma_{ggF}, \sigma_{ZH} / \sigma_{ggF}, \sigma_{ttH} / \sigma_{ggF}, B^{WW} / B^{ZZ}, B^{\gamma\gamma} / B^{ZZ}, B^{\tau\tau} / B^{ZZ}, B^{bb} / B^{ZZ}, \sigma_{ggF}^{7TeV} / \sigma_{ggF}^{8TeV}, \sigma_{VBF}^{7TeV} / \sigma_{VBF}^{8TeV}, \sigma_{WH}^{7TeV} / \sigma_{WH}^{8TeV}, \sigma_{ZH}^{7TeV} / \sigma_{ZH}^{8TeV}, \sigma_{ttH}^{7TeV} / \sigma_{ttH}^{8TeV}$
Coupling ratios	12%	7	$\kappa_{Zg}, \lambda_{Zg}, \lambda_{tg}, \lambda_{WZ}, \lambda_{\gamma Z}, \lambda_{\tau Z}, \lambda_{bZ}$
Couplings, SM loops	74%	6	$\kappa_Z, \kappa_W, \kappa_t, \kappa_\tau, \kappa_b, \kappa_\mu$
Couplings vs mass	55%	2	M, ϵ
Couplings, BSM loops	11%	7	$\kappa_Z, \kappa_W, \kappa_t, \kappa_\tau, \kappa_b, \kappa_g, \kappa_\gamma$
BSM loops only	87%	2	κ_g, κ_γ
Fermion and vector couplings	64%	2	$\lambda_{FV}, \kappa_{VV}$
Up vs down couplings	72%	3	$\lambda_{du}, \lambda_{Vu}, \kappa_{uu}$
Lepton vs quark couplings	79%	3	$\lambda_{lq}, \lambda_{Vq}, \kappa_{qq}$

Production	Loops	Interference	Effective scaling factor	Resolved scaling factor
$\sigma(ggF)$	✓	t - b	κ_g^2	$1.06 \cdot \kappa_t^2 + 0.01 \cdot \kappa_b^2 - 0.07 \cdot \kappa_t \kappa_b$
$\sigma(VBF)$	—	—		$0.74 \cdot \kappa_W^2 + 0.26 \cdot \kappa_Z^2$
$\sigma(WH)$	—	—		κ_W^2
$\sigma(qq/qg \rightarrow ZH)$	—	—		κ_Z^2
$\sigma(gg \rightarrow ZH)$	✓	t - Z		$2.27 \cdot \kappa_Z^2 + 0.37 \cdot \kappa_t^2 - 1.64 \cdot \kappa_Z \kappa_t$
$\sigma(ttH)$	—	—		κ_t^2
$\sigma(gb \rightarrow tHW)$	—	t - W		$1.84 \cdot \kappa_t^2 + 1.57 \cdot \kappa_W^2 - 2.41 \cdot \kappa_t \kappa_W$
$\sigma(qq/qb \rightarrow tHq)$	—	t - W		$3.40 \cdot \kappa_t^2 + 3.56 \cdot \kappa_W^2 - 5.96 \cdot \kappa_t \kappa_W$
$\sigma(bbH)$	—	—		κ_b^2
Partial decay width				
Γ^{ZZ}	—	—		κ_Z^2
Γ^{WW}	—	—		κ_W^2
$\Gamma^{\gamma\gamma}$	✓	t - W	κ_γ^2	$1.59 \cdot \kappa_W^2 + 0.07 \cdot \kappa_t^2 - 0.66 \cdot \kappa_W \kappa_t$
$\Gamma^{\tau\tau}$	—	—		κ_τ^2
Γ^{bb}	—	—		κ_b^2
$\Gamma^{\mu\mu}$	—	—		κ_μ^2
Total width ($B_{\text{BSM}} = 0$)				
Γ_H	✓	—	κ_H^2	$0.57 \cdot \kappa_b^2 + 0.22 \cdot \kappa_W^2 + 0.09 \cdot \kappa_g^2 +$ $0.06 \cdot \kappa_\tau^2 + 0.03 \cdot \kappa_Z^2 + 0.03 \cdot \kappa_c^2 +$ $0.0023 \cdot \kappa_\gamma^2 + 0.0016 \cdot \kappa_{(Z\gamma)}^2 +$ $0.0001 \cdot \kappa_s^2 + 0.00022 \cdot \kappa_\mu^2$

Run-1 Cross section and BR ratio correlations.



$\sigma_i \cdot B^f$ for each channel ($i \rightarrow H \rightarrow f$).



The sensitivity of the Run-I combination allows six of the $\sigma_i \cdot B^f$ to be measured with a precision better than 40%

ggF

$H \rightarrow \gamma\gamma, H \rightarrow ZZ, H \rightarrow WW$

VBF

$H \rightarrow \gamma\gamma, H \rightarrow WW, H \rightarrow \tau\tau$

Production process	Measured significance (σ)	Expected significance (σ)
VBF	5.4	4.6
WH	2.4	2.7
ZH	2.3	2.9
VH	3.5	4.2
<i>ttH</i>	4.4	2.0
Decay channel		
$H \rightarrow \tau\tau$	5.5	5.0
$H \rightarrow bb$	2.6	3.7

Factor of $\sqrt{2}$ improvement in sensitivity from ATLAS+CMS combination

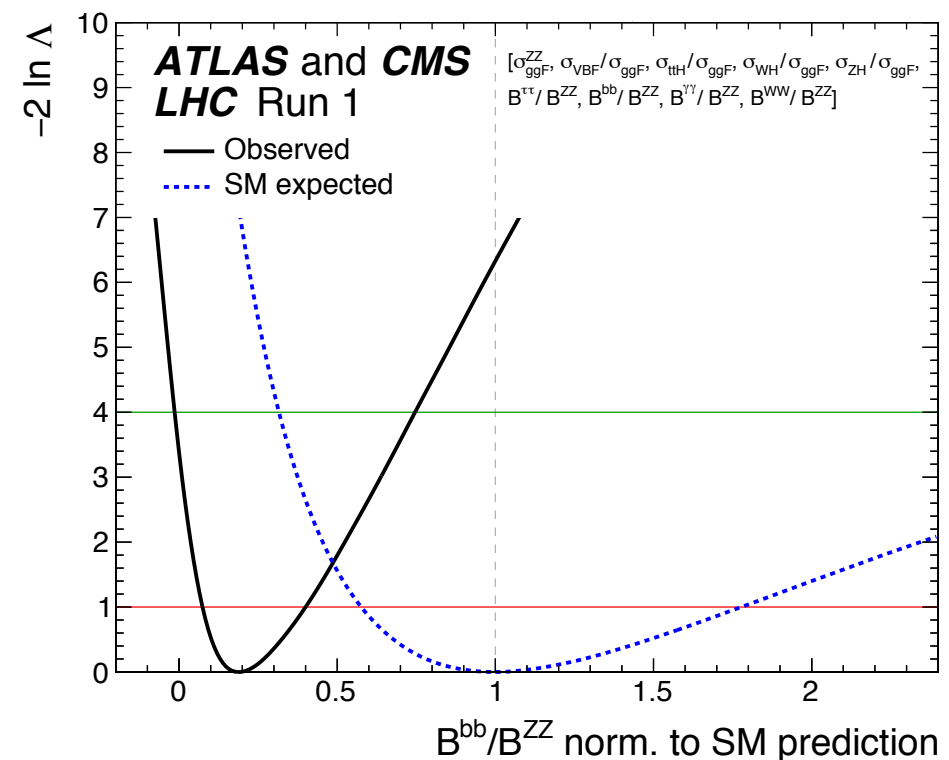
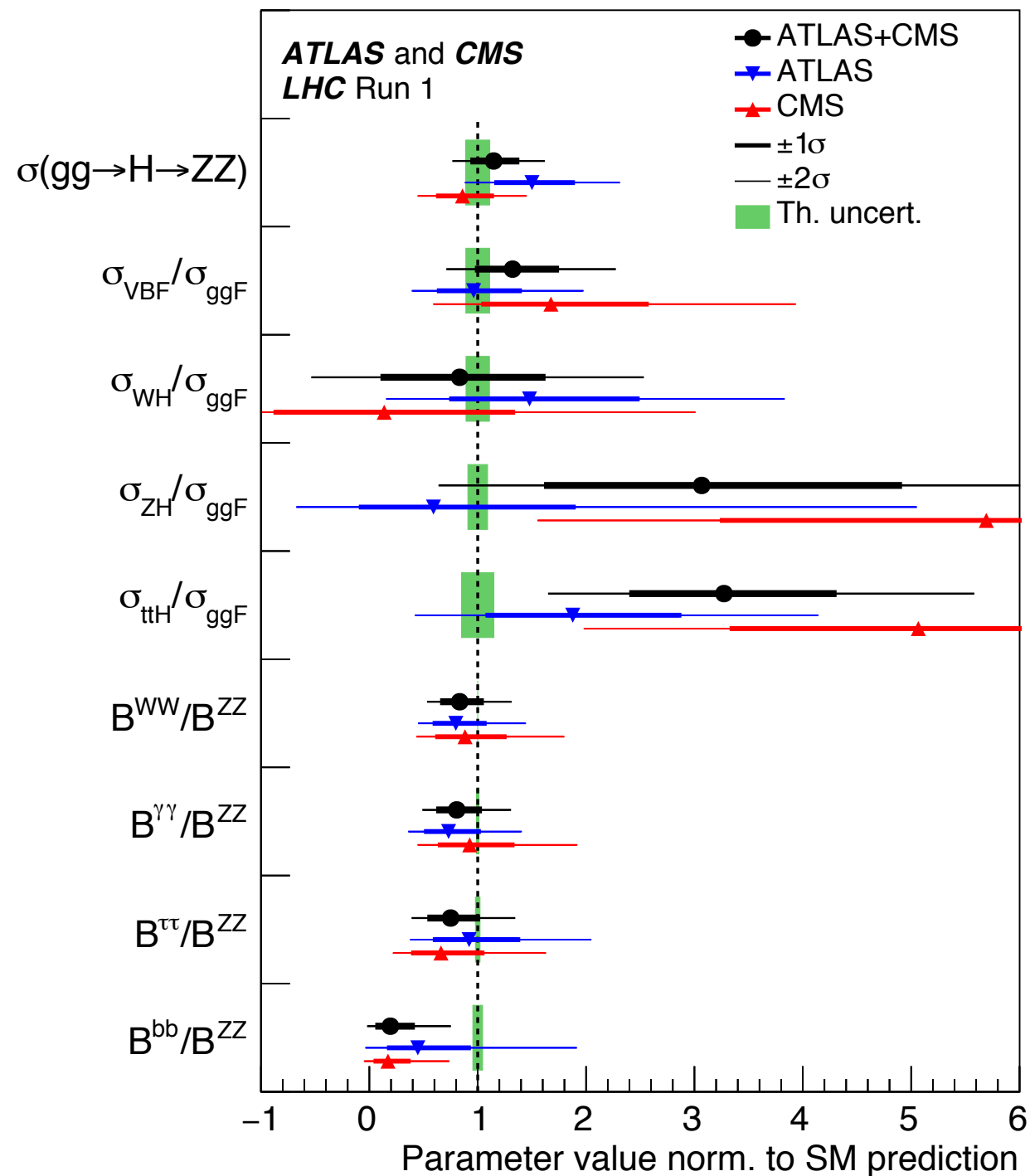
- Combined **$>5\sigma$** significance provides **observation of VBF production and $H \rightarrow \tau\tau$ decay**
- **$>3\sigma$** significance for **VH production**
- **4.4σ** significance for ***ttH* (2.3σ excess relative to SM)**

$$\sigma_i \cdot B^f = \sigma(gg \rightarrow H \rightarrow ZZ) \cdot \left(\frac{\sigma_i}{\sigma_{ggF}} \right) \cdot \left(\frac{B^f}{B^{ZZ}} \right)$$

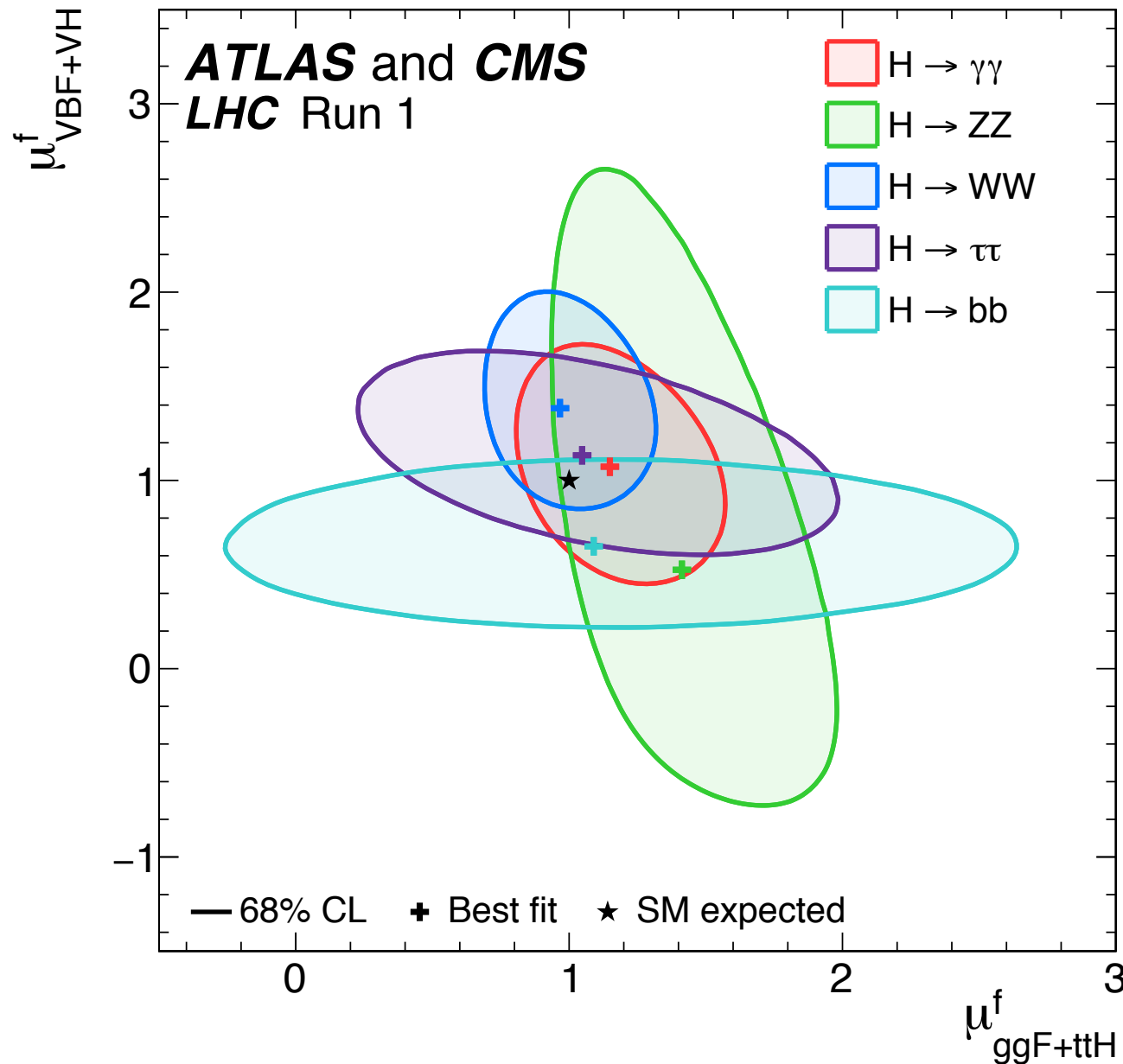
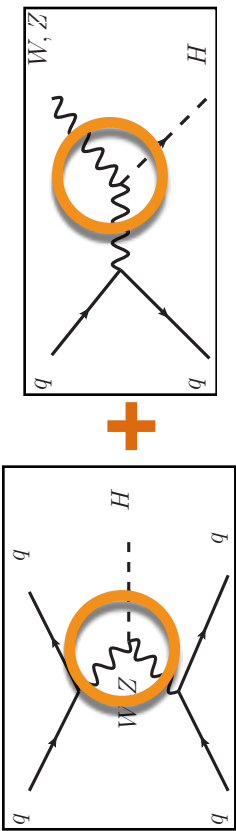
$\frac{\sigma_{ttH}}{\sigma_{ggF}}$ ratio of **3.3 ± 1.0 (3σ excess)** relative to SM (mainly from multi-lepton)

$\frac{\sigma_{ZH}}{\sigma_{ggF}}$ ratio of **3.2 ± 1.7** relative to SM (slightly milder excess)

$\frac{B^{bb}}{B^{ZZ}}$ ~**2.5σ** deficit relative to SM (in current parameterization, high values for $\sigma_{ttH}/\sigma_{ggF}$ and σ_{ZH}/σ_{ggF} induce a low $H \rightarrow bb$)



Production μ by decay channel.

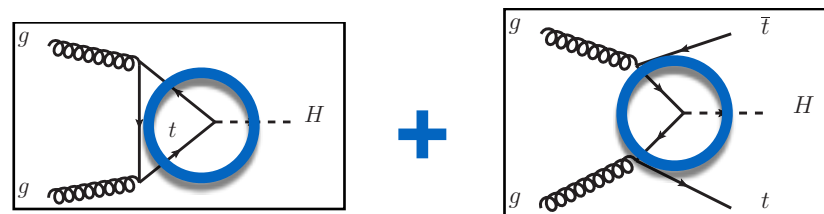


$$\mu_i^f = \frac{\sigma_i \cdot B^f}{\sigma_i^{SM} \cdot B_{SM}^f}$$

Parameterization using **two production signal strengths (*i*)**, one for **fermions** and one for **bosons**:

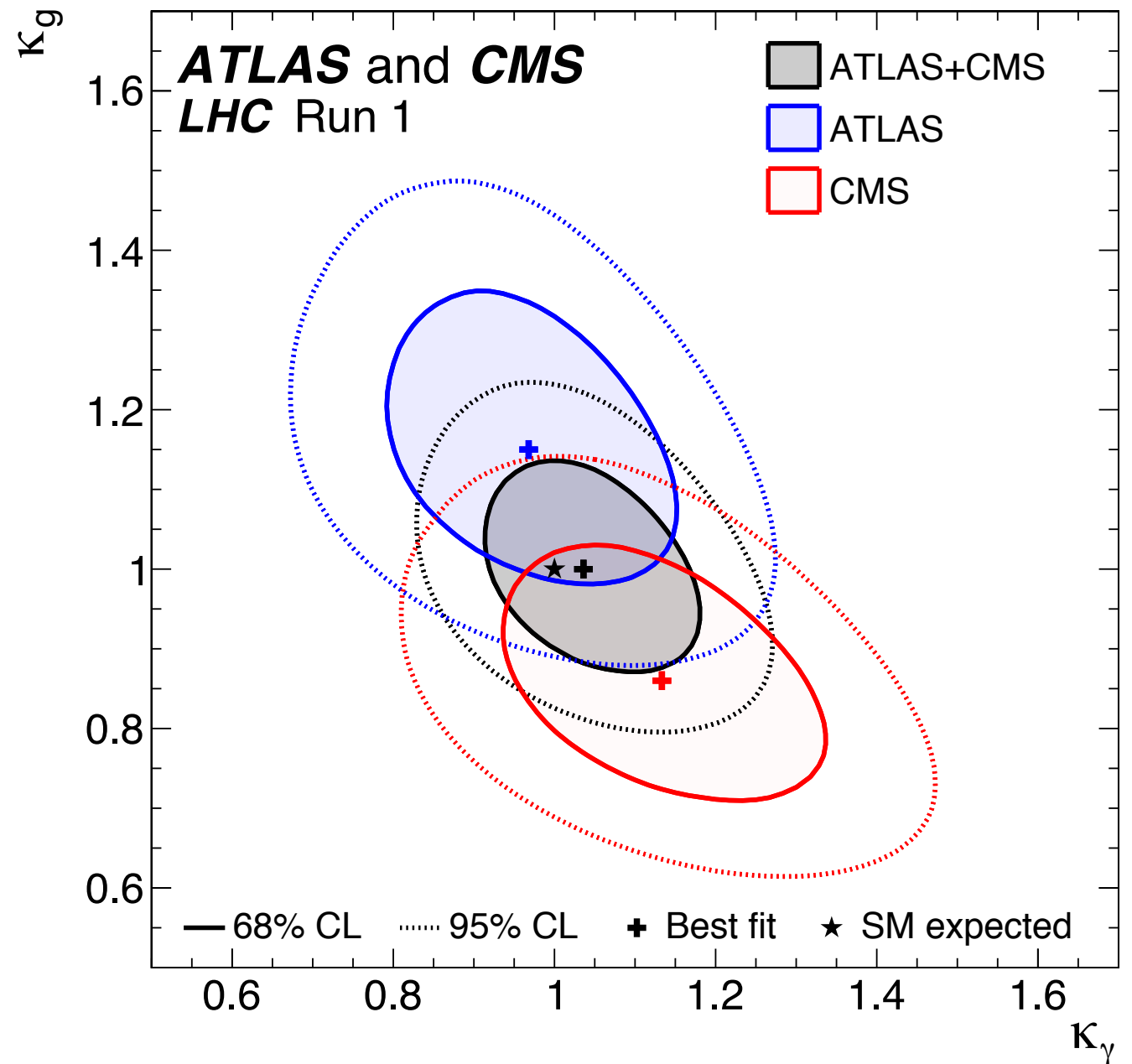
$$\mu_{ggF+ttH}^f \text{ VS. } \mu_{VBF+VH}^f$$

Good agreement with SM prediction for all decay channels



$$\Gamma_H = \frac{\kappa_H^2 \Gamma_H^{SM}}{1 - B_{BSM}}$$

- No BSM decays ($B_{BSM} = 0$)
- All the couplings to SM particles are the same as in the SM
- Only the ggF production and $\gamma\gamma$ decay loops are allowed to be affected by the presence of additional particles
- Only free parameters κ_γ and κ_g , with all other coupling modifiers fixed to their SM values



p -value of the compatibility between the data and the SM predictions is 82%

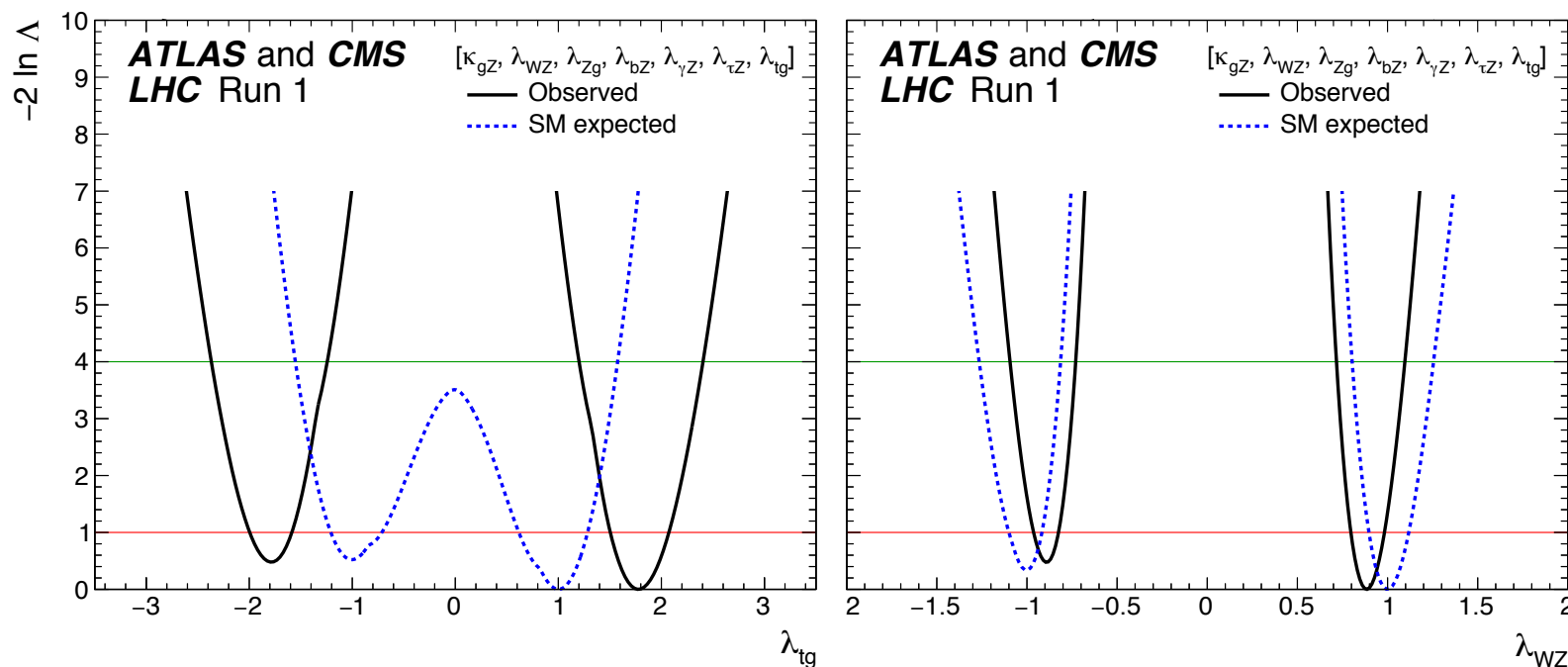
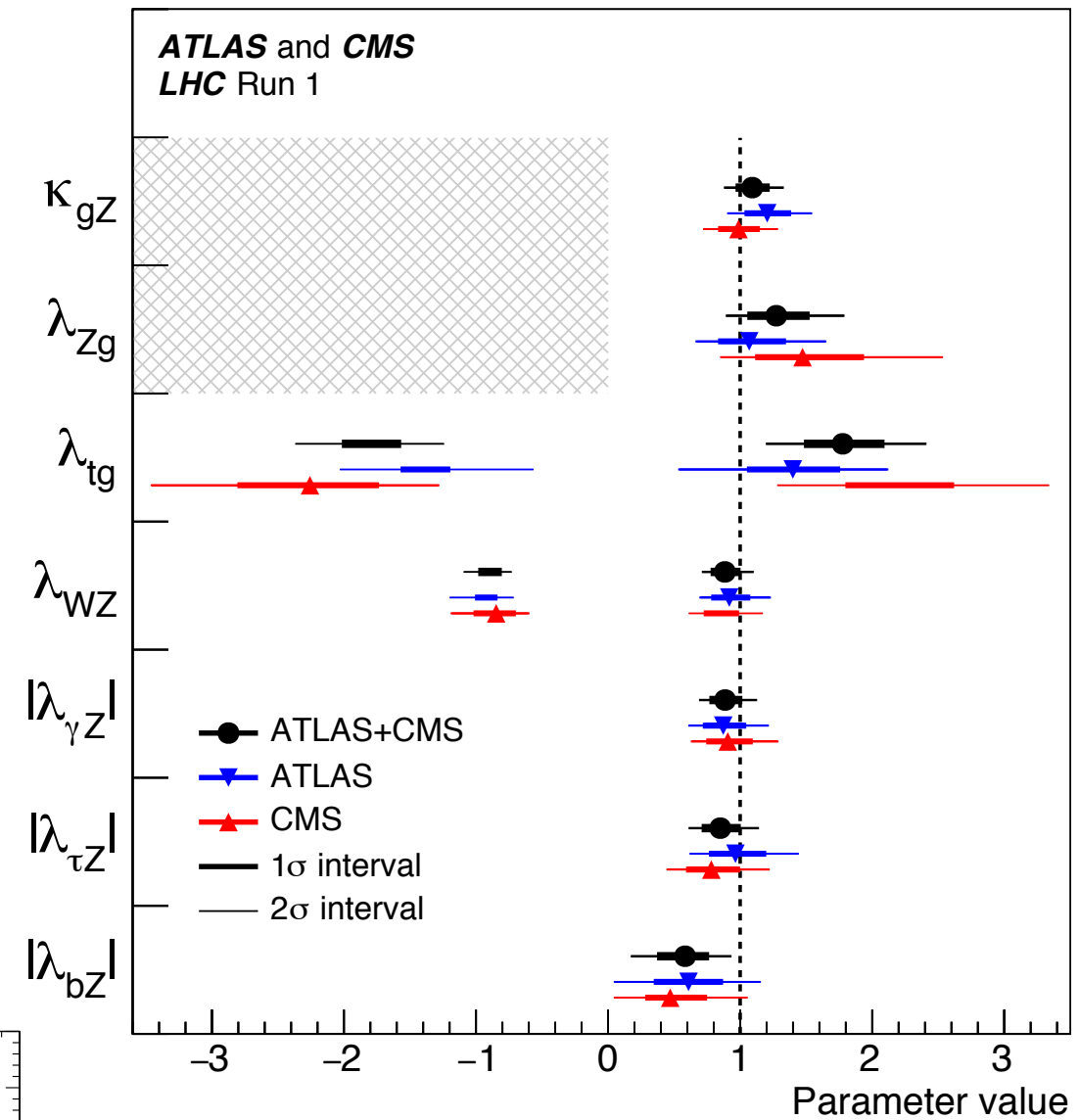
Conversion of signal strength ratios into κ -framework using:

$$\lambda_{ij} = \frac{\kappa_i}{\kappa_j}$$

Cross section times branching fraction for the $gg \rightarrow H \rightarrow ZZ$ channel is parameterized as a function of:

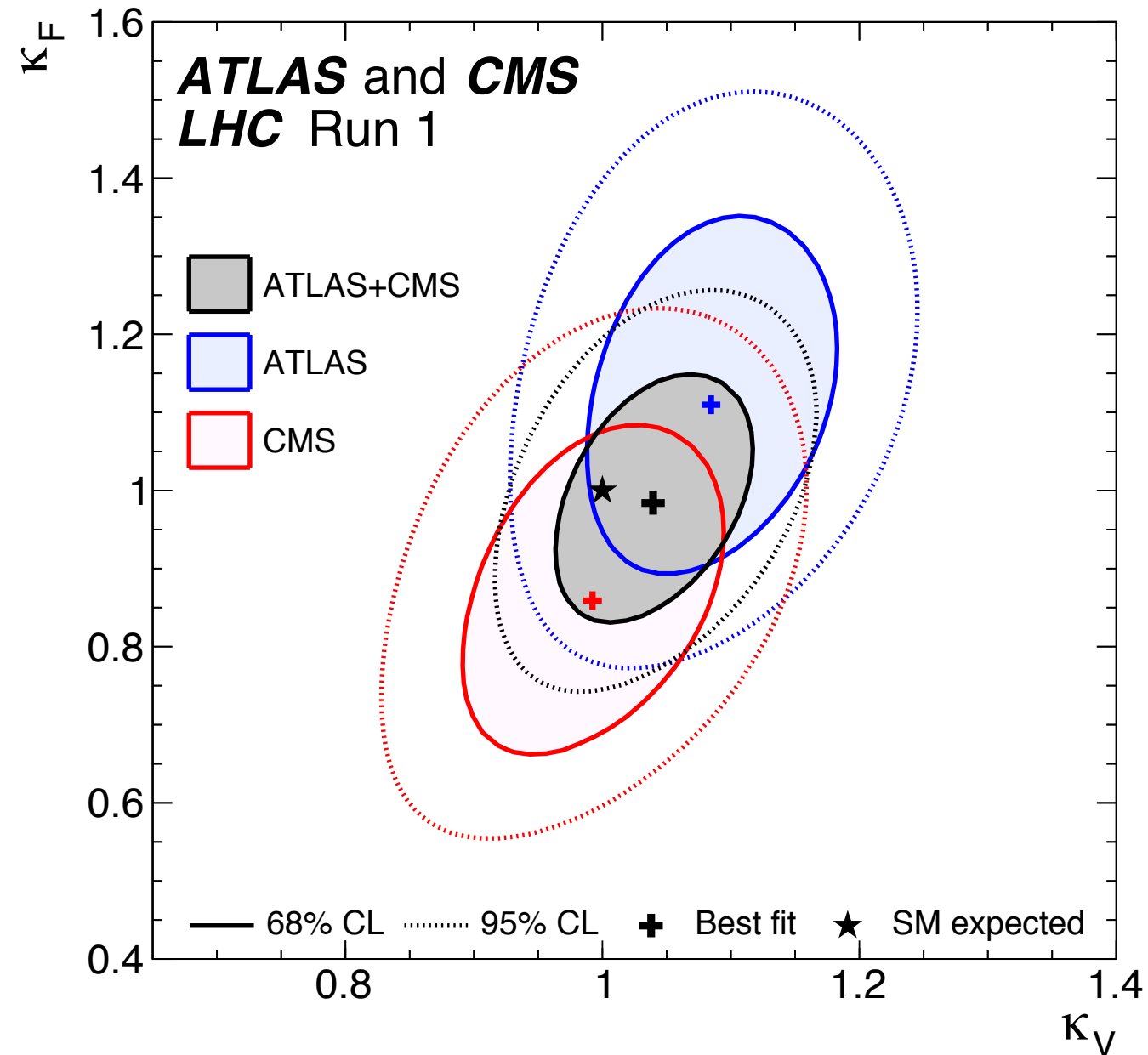
$$\kappa_{gZ} = \frac{\kappa_g \kappa_Z}{\kappa_H}$$

then all other κ 's can be determined



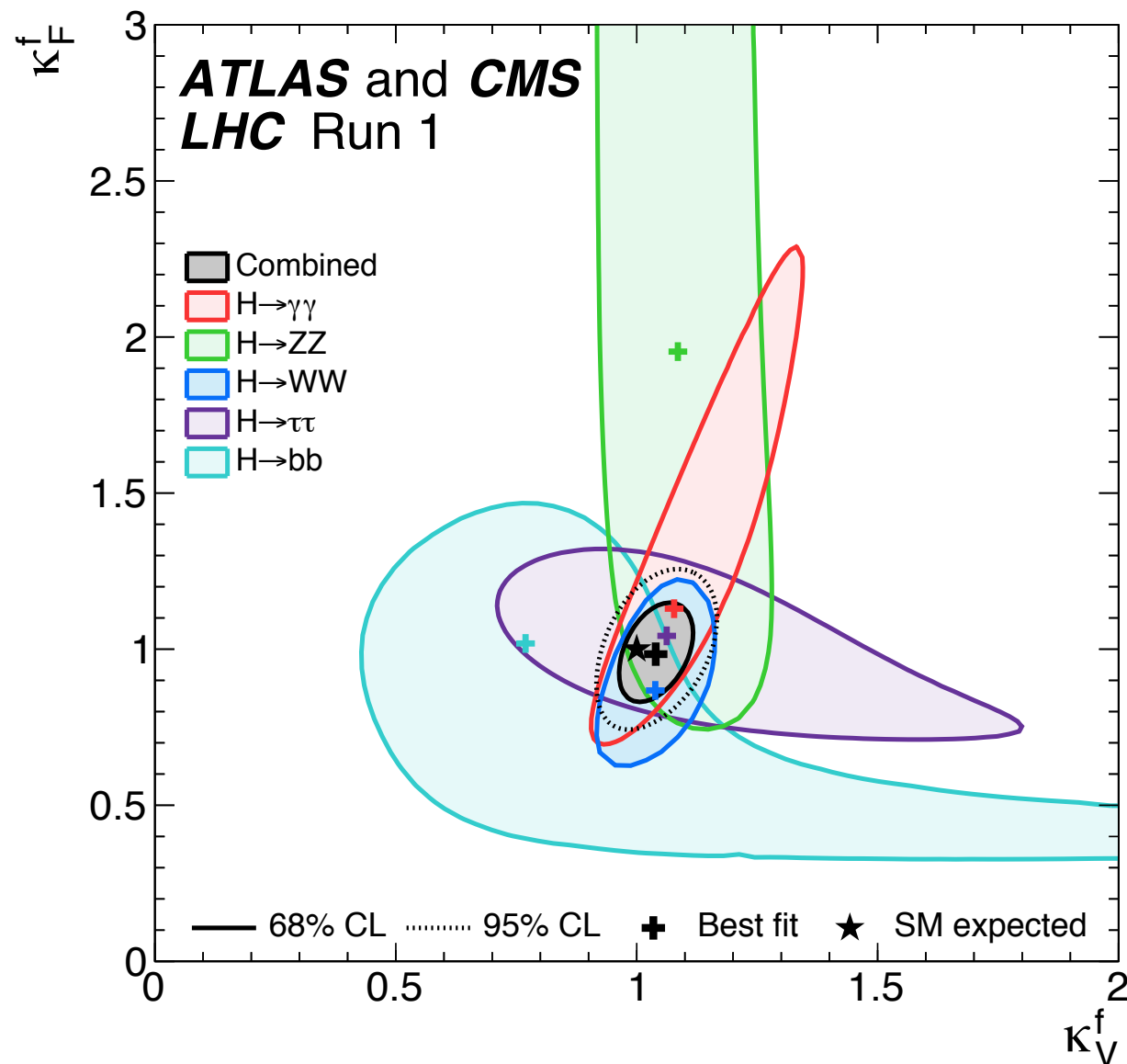
Negative ranges allowed for λ_{WZ} and λ_{tg} to illustrate possible interference effects due to $ggZH$ or tH production

Best fit > 0 , but limited sensitivity to interference terms

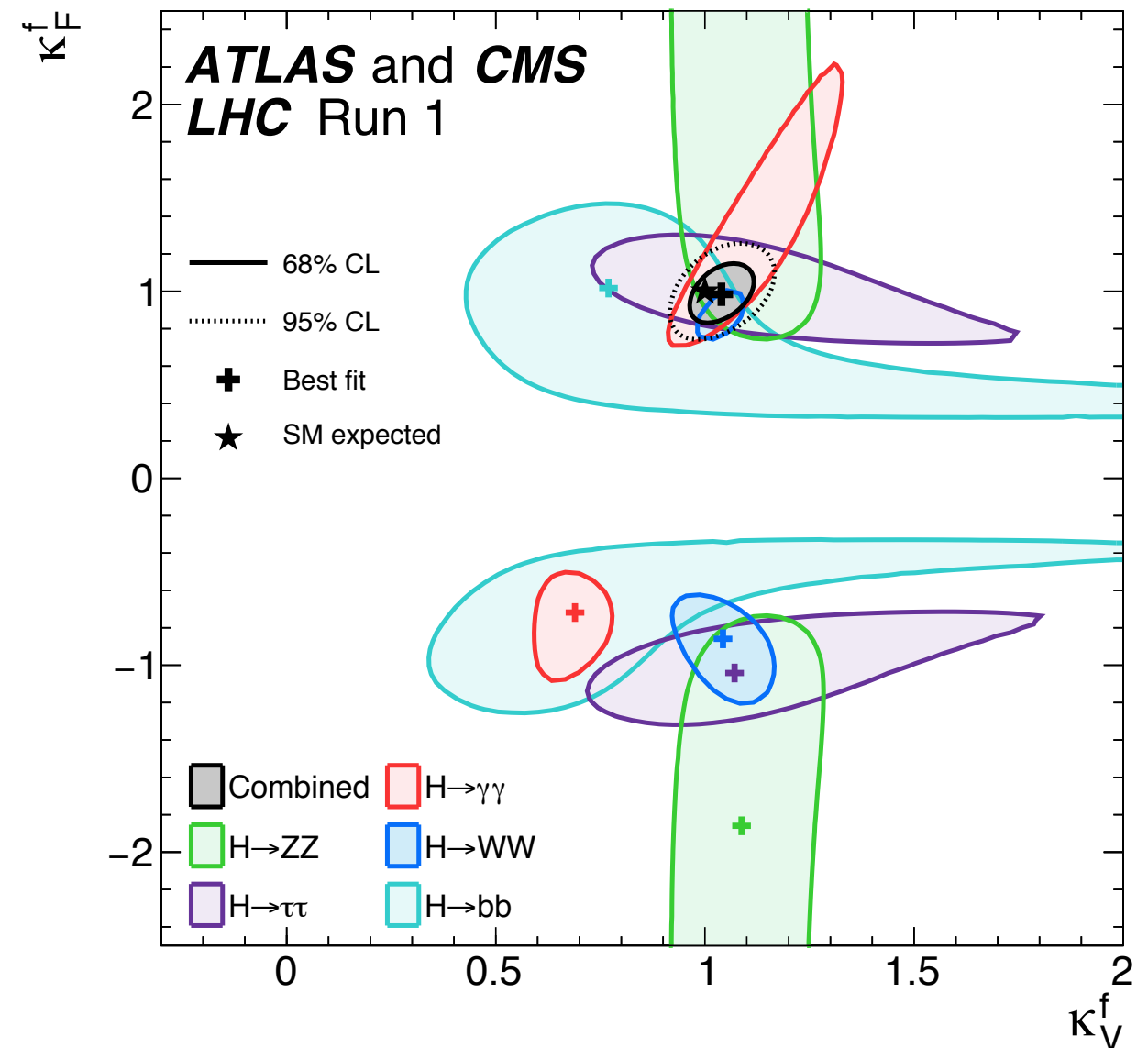


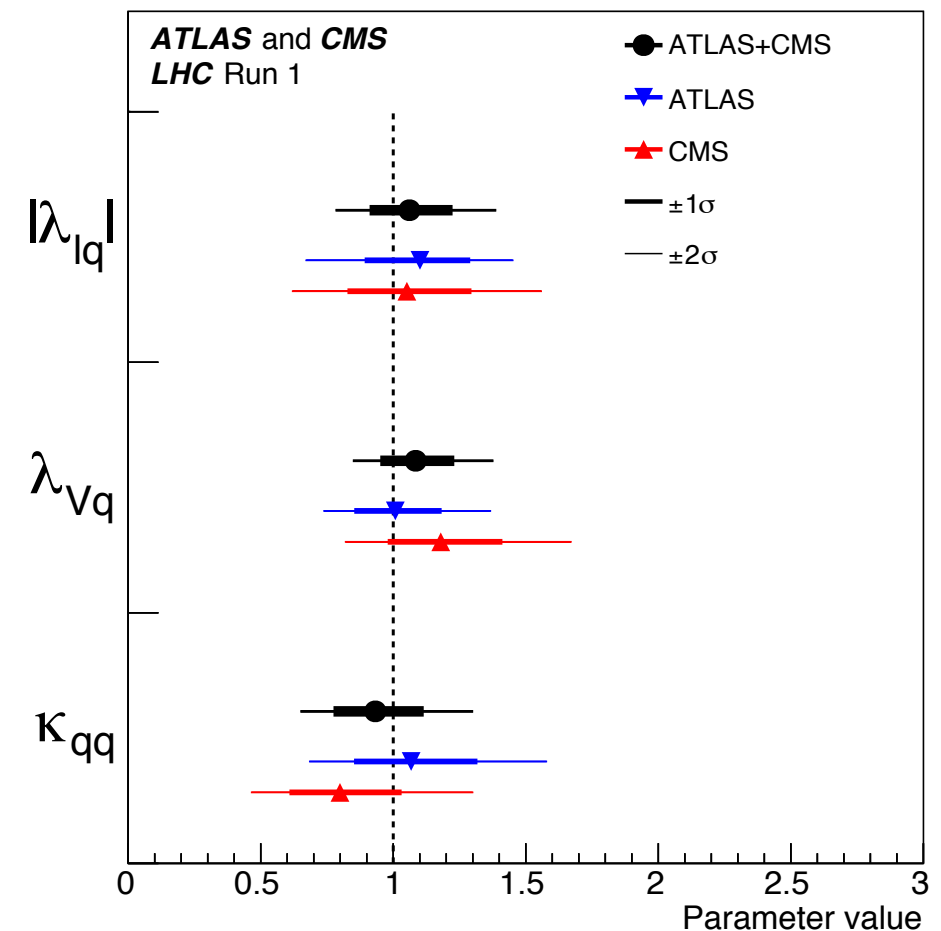
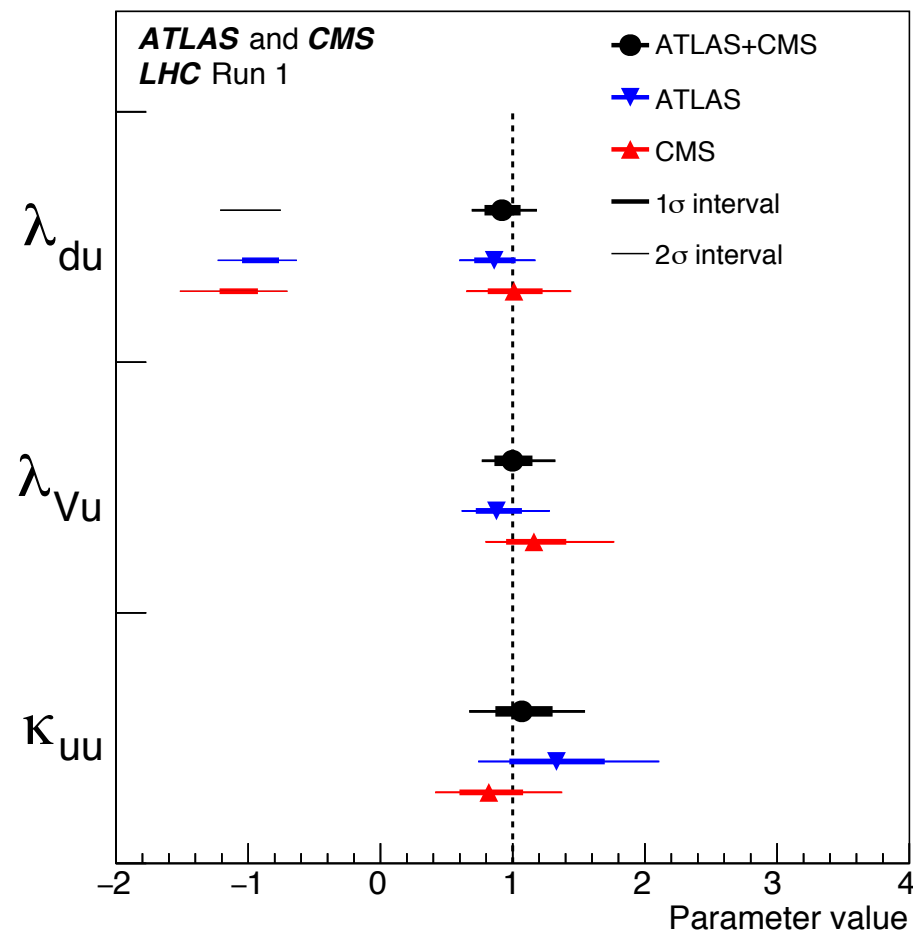
- SM Higgs couplings to fermions and boson very different
***Yukawa* vs $D\mu \rightarrow \kappa_F$ vs κ_V**
- κ_F, κ_V in agreement with SM
- $\kappa_F \times \kappa_V < 0$ excluded at almost **5 σ**

Likelihood contours at 68% CL in the (κ_F^f, κ_V^f) plane for the combination and for the individual decay channels as well as for their global combination, all κ 's are assumed to be positive



Likelihood contours at 68% and 95% CL in the (κ_F^f, κ_V^f) plane for the individual decay channels and also the combination, with no assumption about the sign of the coupling modifiers





- ***u-type & d-type*** quarks could couple to different fields
- Test potential variations of $\lambda_{ud} = \frac{\kappa_d}{\kappa_u}$
- ***Charged leptons*** have same couplings as d-quarks for λ_{ud}
- test the variation of coupling to leptons vs quarks $\lambda_{lq} = \frac{\kappa_l}{\kappa_q}$

All ratios consistent with unity

Couplings with BSM loops and new decays.

